Summer 6-6-1958

Design of an Experiment to Separate Specular and Scattered Radar Returns

Robert B. Glascock

DESIGN OF AN EXPERIMENT - GLASCOCK

DESIGN OF AN EXPERIMENT TO SEPARATE SPECULAR AND SCATTERED RADAR RETURNS

By

Robert B. Glascock

A Thesis

Submitted in Partial Fulfillment of the

Requirements for the Degree of

Master of Science in Electrical Engineering

The University of New Mexico

1958

This thesis, directed and approved by the candidate's committee, has been accepted by the Graduate Committee of the University of New Mexico in partial fulfillment of the requirements for the degree of

MASTER OF SCIENCE

E H Castetter
DEAN

June 3, 1958
DATE

Thesis committee

R. F. Adams
CHAIRMAN

Bo M. Tanner

A H Knuhmann

Table of Contents

DESIGN OF AN EXPERIMENT TO SEPARATE SPECULAR AND SCATTERED RADAR RETURNS

1.0 Introduction

This paper describes the design of a radar experiment that will be conducted by the U. S. Naval Research Laboratory at Washington, D.C. The proposed experiment and the background of the problem are discussed in this section and the theoretical background, experimental background, and other design considerations are discussed in later sections.

1.1 Background of the Problem. Radar echoes have been known to consist of a specular (mirror type) reflection and a scattered component described by a reflection coefficient and scattering cross-section per unit area for the ground.[1] The problem has been to separate these two parameters of the ground so that for any radar altimeter system the return may be accurately predicted. Radar return measurements taken by Sandia Corporation in recent years have been made in such a manner that the effects of reflection and scattering cannot be separated with any confidence, especially at angles near vertical incidence.

---

[1] R. K. Moore and C. S. Williams, Jr., "Radar Return at Near Vertical Incidence." Proc. IRE., Vol. 45, No. 2, Feb. 1957, pp. 228-238.

The experiment discussed in this paper has been designed to gather data so that the ground parameters may be separated with much more accuracy and confidence. The results of the design are given in the next paragraph.

1.2 Results of the Experiment Design Study. This study has shown that data which will allow the separation of the ground parameters can be obtained in the following manner.

A pulsed radar in an airplane will illuminate the terrain alternately with two antennas with different beam widths. One antenna will be quite narrow and the other rather wide. The narrow antenna will receive signals due almost entirely to specular reflections while the wide-beam antenna will receive signals due to both specular and scattered return. The power returned to the narrow beam can be (under certain conditions to be described later) subtracted from the power returned to the wide beam to give the power due to scattering. With this information the scattering cross-sections of the ground can be deduced.

The system parameters for this experiment are given in Table 1 where the particular section that discusses the selection of each is listed.

2.0 Theoretical Background.

Radar return has been the object of a great deal of study for more than a decade, but most of the work has been for

Table 1

Parameter	Selection	Discussed In:
Frequency	3280 mcps	4.22
Pulse width and shape	0.25 sec (see Fig. 1)	4.23
Narrow beam antenna pattern Wide beam Antenna pattern	See Fig. 2	4.21
Receiver Bandwidth	5 MC	4.24
Altitudes	4,000; 7,000; 12,000 Any one or combination	5.20
PRF	100 to 200 cps	5.7
Targets	Farmlands, residential, commercial, water, woods - summer and winter	5.1
Aircraft speed	Approx. 150 mph	5.8
Transmitted power	4000' - 1.8 w 7000' - 8.5 w 12000' - 40.5 w	4.25
Block diagram	See Fig. 3	5.6

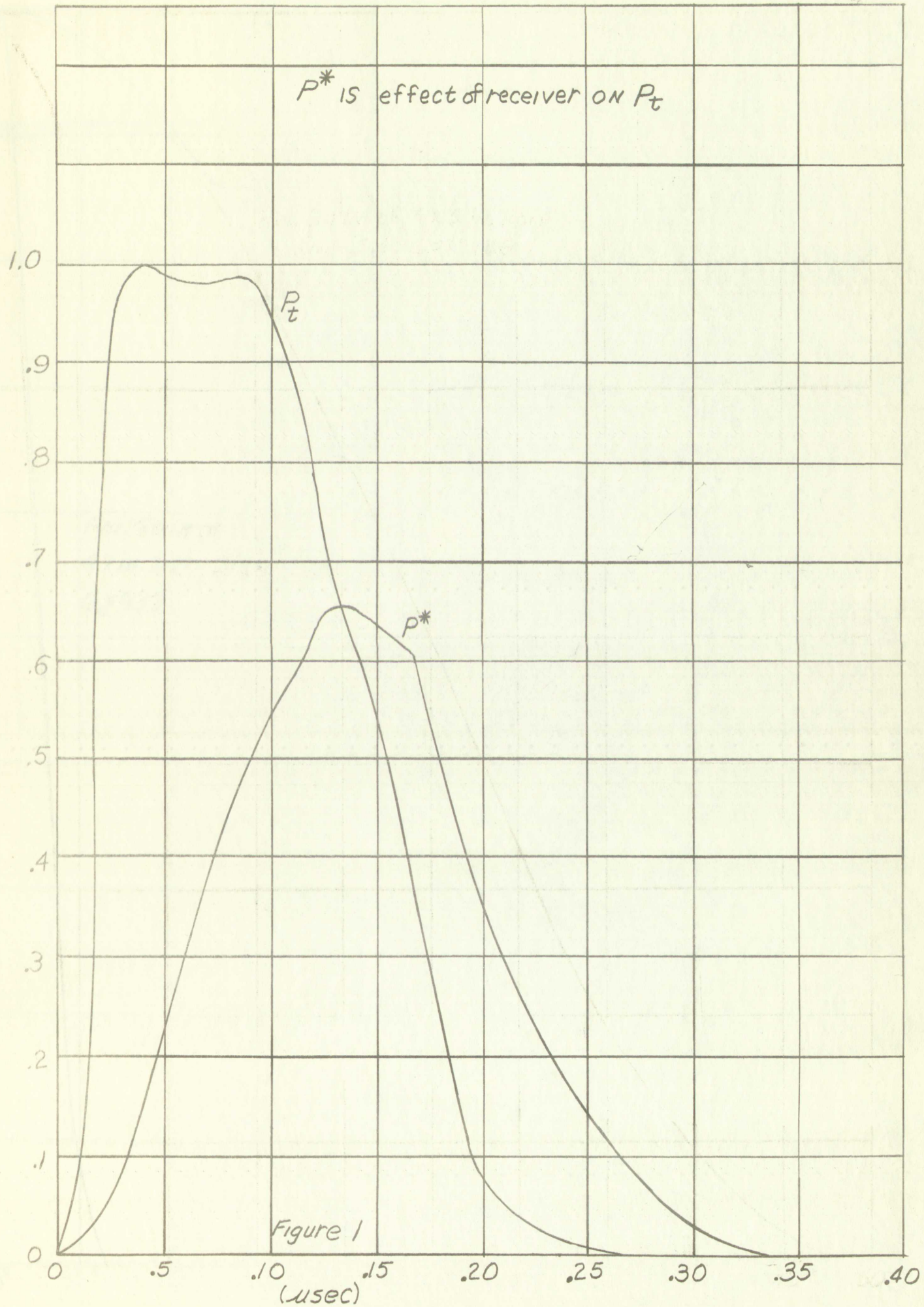
P* is effect of receiver on Pt
Pt
P*
1.0
.9
.8
.7
.6
.5
.4
.3
.2
.1
0
0
.5
.10
.15
.20
.25
.30
.35
.40
(usec)

Figure 1

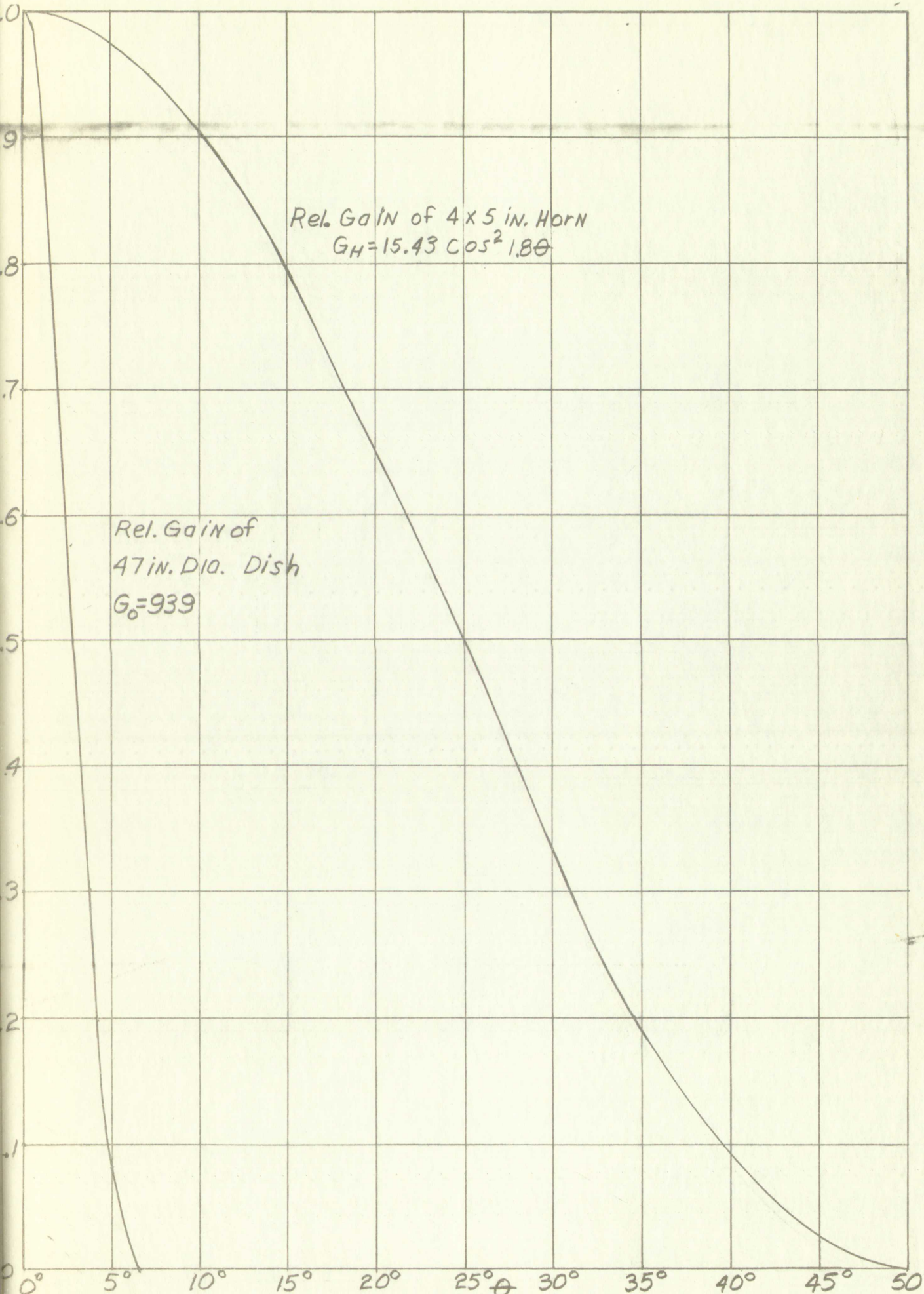
Rel. Gain of 4 x 5 in. Horn
$G_H = 15.43 \cos^2 1.8\theta$
Rel. Gain of
47 in. Dia. Dish
$G_o = 939$
1.0
.9
.8
.7
.6
.5
.4
.3
.2
.1
0
0°
5°
10°
15°
20°
25°
θ
30°
35°
40°
45°
50°

Figure 2

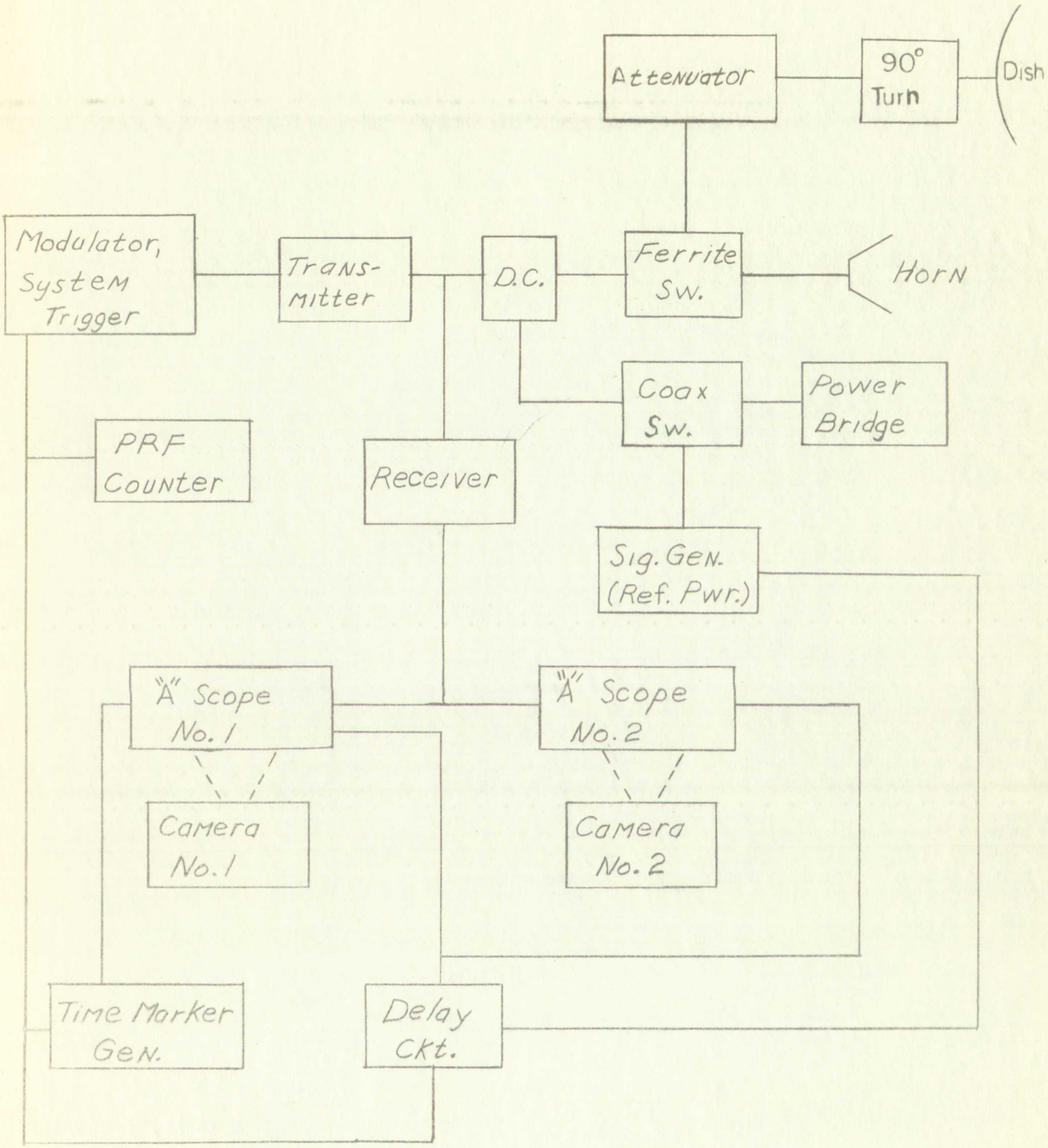

Block Diagram

Figure 3

angles near grazing incidence and almost no data have been taken for angles near vertical incidence. The data that have been taken for angles near vertical incidence have been reduced in terms of a scattering cross-section per unit area and a reflection coefficient. Another method that describes the return in terms of the statistical variations of the ground about a mean ground level has been proposed by Davies and Moore.[2,3] However, some of the assumptions made by Davies do not hold at angles near vertical incidence. Radar return for these two models will be discussed in the following two sections with an extension on Davies' theory.

2.1 Radar Return at Near-Vertical Incidence. The return due to specular reflection is given by a single term, but the return due to scattering involves an integral. These two types of return will be discussed separately.

2.11 Radar Return Due to Specular Reflection. The return due to specular power can be developed on an image basis to give:

$$P_r(t) = \frac{P_t(t-\frac{2h}{c})G^2(0)K^2\lambda^2}{64\pi^2h^2} \qquad (1)$$

---

[2]H. Davies, "Reflection of Electromagnetic Waves from a Rough Surface", IEE Monograph #90, (1954).

[3]R. K. Moore, "Resolution of Vertical Incidence Return into Random and Specular Components", UNM Exp. Sta. Tech Report EE-6, (July, 1957) Presented before the URSI Meeting, Washington, D. C., (May, 1957).

where $P_r(t)_{sp}$ is the specular power returned, $P_t\ (t-\frac{2h}{c})$ is the transmitted power, G(0) is the gain to a point directly below the radar, λ is the wavelength, h is the distance from the radar to the ground, and K is the Fresnel voltage reflection coefficient. It should be noted that, after an area a few Fresnel zones wide is illuminated, essentially specular power is returned to the radar and this return is not dependent on any additional area illuminated.[4]

2.12 Radar Return Due to Scattering. The process of scattering is one wherein the ground reradiates the incident power in all directions, but with some directivity.[5] The development given in the reference will be repeated for convenience, but not in the original detail.

Consider an airplane flying over the terrain with a pulsed radar that periodically illuminates the ground directly below and out to some angle Θ, where the area illuminated is defined by the antenna pattern of the radar and the pulse duration. The return from any scatterer associated with a small

---

[4]Paul Drude, Theory of Optics, Longman, Green & Co. (London, 1913) p. 164.

[5]Moore and Williams, op. cit. (Ref. 1)

illuminated area, ΔA, will now be developed with the geometry illustrated in Figure 4.

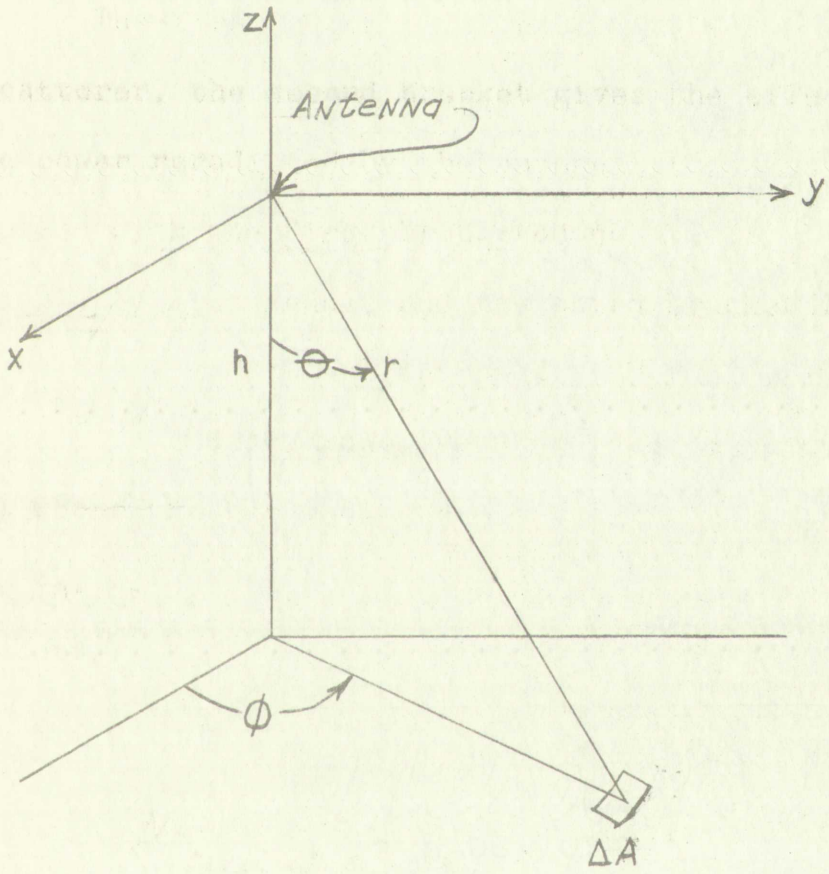

Figure 4

The return from any scatterer, $P_r(t)$, will be:

$$P_r(t) = \left[\frac{P_t(t-\frac{2r}{c})G_N}{4\pi r_N^2}\right]\left[\frac{\sigma_N}{4\pi r_N^2}\right]\left[\frac{G_N \lambda^2}{4\pi}\right] \qquad (2)$$

Where $P_r(t)$ is the returned power from the nth scatterer,

r is the range to the nth scatterer,

G_N is the gain to the nth scatterer,

σ_N is the scattering cross-section of the nth scatterer,

and λ is the wavelength of the radar.

The first bracket is the power density incident at the nth scatterer, the second bracket gives the effect of the ground on the power reradiated by the antenna at the antenna (and when multiplied with the first bracketed quantity gives the power density back at the antenna), and the third bracket is the effective receiving aperture of the antenna.

The average power returned due to scattering is given in (3) where the bar indicates that any point in the returned pulse, t_n, is an average of the values at the time, t_n, in all of the pulses.

$$\overline{P_r(t)} = \sum_{N=1}^{N} \frac{P_t(t-\frac{2r}{c}) G_N^2 \lambda^2 \sigma_N}{64\pi^3 r^4} \qquad (3)$$

The notation, $P_t\ (t-\frac{2r}{c})$, expresses the pulse power as if the pulse had started when the leading edge touched the ground, as shown in Figure 5.

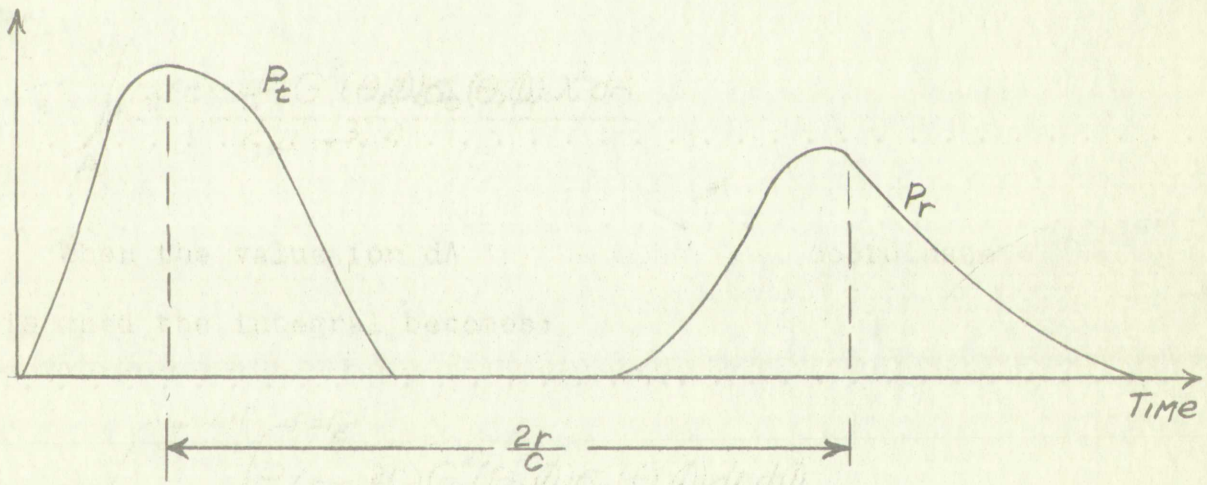

Figure 5

The scattering cross-section is a quantity that would be very difficult to evaluate for each scatterer on the ground and, for this reason, a new quantity, σ_0, is defined. The definition for σ_0 is given in (4).

$$\sigma_0 = \frac{\sigma_N}{\Delta A} \tag{4}$$

The quantity in (4) is the scattering cross-section per unit area where the unit area may contain several scatterers.

The summation given in (3) must be multiplied by ΔA when (4) is substituted into (3), and the sum will become an integral when the increment of area is allowed to approach zero, resulting in:

$$\overline{P_r(t)}_{SC} = \int_A \frac{P_t(t-\frac{2r}{c})G^2(\theta,\phi)\sigma_0(\theta,\phi)x^2 dA}{64\pi^3 r^4} \tag{5}$$

When the value for dA in the spherical coordinate system is used the integral becomes:

$$\overline{P_r(t)}_{SC} = \int_{\phi=0}^{\phi=2\pi} \int_{r=r_1}^{r=r_2} \frac{P_t(t-\frac{2r}{c})G^2(\theta,\phi)\sigma_0(\theta,\phi)dr\,d\phi}{64\pi^3 r^3} \tag{6}$$

The integration on ϕ can be readily performed which gives a value of 2π on the outside of the integral, if $G^2(\theta)$ and $\sigma_0(\theta)$ are assumed to have circular symmetry with respect to a vertical axis from the radar to the ground.

This integral gives the power received due to scattering. The total power returned is given by the sum of (1)

and (6), the power due to specular and scatter, as shown in (7).

$$\overline{P_r(t)} = \frac{P_t(t-\frac{2h}{c})G^2(0)K^2\lambda^2}{64\pi^2h^2} + \int_{r=r_1}^{r=r_2} \frac{P_t(t-\frac{2r}{c})G^2(\theta)\sigma_o(\theta)\lambda^2 dr}{32\pi^2 r^3} \qquad (7)$$

The gain and scattering cross-section per unit area are given as functions of the angle θ since this variable is not altitude dependent.

2.2 Resolution of Return into Specular and Scattered Components. The basis[6,7] for this method of describing the return uses the statistics of the fluctuations of the ground level about some mean value. The return is broken up phasorially into a component with phase that of an area element at the mean level and a component that contains the effect of the random distributions of the heights of these area elements around the mean level of the ground. The distribution of the heights of the area elements is assumed to follow the normal law, which results in a normal distribution of the phases associated with the returns from the various area elements intead of the usual assumption of a uniform distribution of the phases.

---

[6] R. K. Moore, op. cit. (Ref. 3).

[7] H. Davies, op. cit. (Ref. 2).

Both of these references develop the return in terms of the standard deviations of the ground fluctuations and show how the specular component decreases as the standard deviation of the fluctuations increases. However, Davies makes some assumptions that are not always valid near vertical incidence. Moore does not make the assumptions that make Davies' development invalid at vertical incidence, but obtains an integral that cannot be evaluated except by numerical methods.

The experiment that NRL will conduct should verify Moore's and Davies' theories (except at vertical incidence in the case of Davies' theory). The experiment will also give better information on the variation of the scattering cross-section with angles of incidence. The data taken by Sandia could also be fitted with these curves since the general shape of the variations will be known. Comparison will be of particular interest where NRL flights are made over old Sandia targets.

The attempts to reduce (in terms of the specular-scatter combination) the large quantities of data taken by Sandia Corporation will be discussed to give a better insight into the problems involved in the separation of the scattering cross-section and reflection coefficient.

3.0 Experimental Background.

A great amount of data has been taken in the Sandia Corporation terrain return program, and a great deal of effort

has been spent in its analysis. It has been evident since introduction of the specular-scatter theory that separation of existing data would be difficult. The method used by Sandia Corporation to take data and the method used in the reduction of the data are discussed here to illustrate the problems in their program and how this experiment will overcome these difficulties.

3.1 Experimental Program Conducted by Sandia Corporation. Sandia used a pulsed radar in a C-47 with a broad beam antenna to transmit and receive narrow pulses of the order of 0.1 to 0.2μ sec in width. The calibrations of the transmitted power varied as much as 7 db between ground and data run calibrations and they were not improved until inflight calibrations were made.[8] The data collected after inflight calibrations were started are more accurately calibrated with respect to the transmitted power, since the fluctuations are no greater than 2 db, but the ground parameters cannot be readily separated since the measurements were made with a wide-beam antenna so the power returned due to the specular and scattering processes was combined.

---

[8]F. Janza and R. West, "Accurate Radar Attenuation Measurements Achieved by Inflight Calibration," IRE Trans. on Instrumentation, pp. 23-30, (Oct., 1955).

The pulse-to-pulse oscilloscope photos were reduced by the Physical Science Laboratory at New Mexico College of A. & M. A., State College, New Mexico. The method used by PSL is discussed in the next section which points out some possible errors in the reduction of the data.

3.2 Reduction Procedures Applied to Sandia Corporation Data. The reduction of the Sandia data was performed by removing the scattering cross-section per unit area from the integral of equation (6) as an average of the values between the limits of the integral. The value of the average scattering cross-section at any time, t_n, in the return was found by dividing the average power returned by the value of the integral at the same time. This did not account for the power due to the specular component so an exponential, $A\exp(-B\theta)$ was fitted to the values of the average scattering cross-section. The curve fitting was applied only to those points that did not have a specular component added to the scattered power. The exponential was chosen because it was easy to use, and at the time no better information was available on the variation of $\sigma_o(\theta)$ with the angles of incidence. Such a fit is shown in Figure 6.

It is interesting to combine the power due to scattering and specular return into a single integral. The identity $h = r \cos \theta$, and the properties of the δ function listed

below are needed.

$$\delta(t) = \infty \quad t = 0$$
$$= 0 \quad t \neq 0$$
$$\int_{-\infty}^{\infty} \delta(t)\,dt = 1$$
$$\int_{-\infty}^{\infty} f(t)\,\delta(t-\tau)\,dt = f(\tau) \tag{8}$$

The proper substitutions of the quantities in (8), and the identity into (7) will give the expression below for the total power returned as a single integral.

$$\overline{P_r(t)} = \lambda^2 \int_{r_1}^{r_2} \frac{P_t(t - \frac{2r}{c})\,G^2(\theta)}{32\pi^2 r^3} \left[\frac{r^3 K^2 \delta(h-r)}{h^2} + \sigma_o(\theta) \right] dr \tag{9}$$

The bracketed quantity can be reduced further by using the properties of the δ function to substitute h^3 for r^3.

The quantity in brackets in the above expression, defined as $\overline{\sigma_o'(\theta)}$, is the value that PSL has deduced from the data as a first approximation to the average scattering cross-section. The δ function in the brackets illustrates why the values of the returned power that contain the specular component cannot be used in the reduction of the average scattering cross-section.

Curves for the actual average scattering cross-section, $\sigma_o(\theta)$, the value reduced by PSL, $\overline{\sigma_o'(\theta)}$, and the exponential used in the curve fitting process, $\overline{\sigma_o(\theta)}$, are shown in Figure 6.

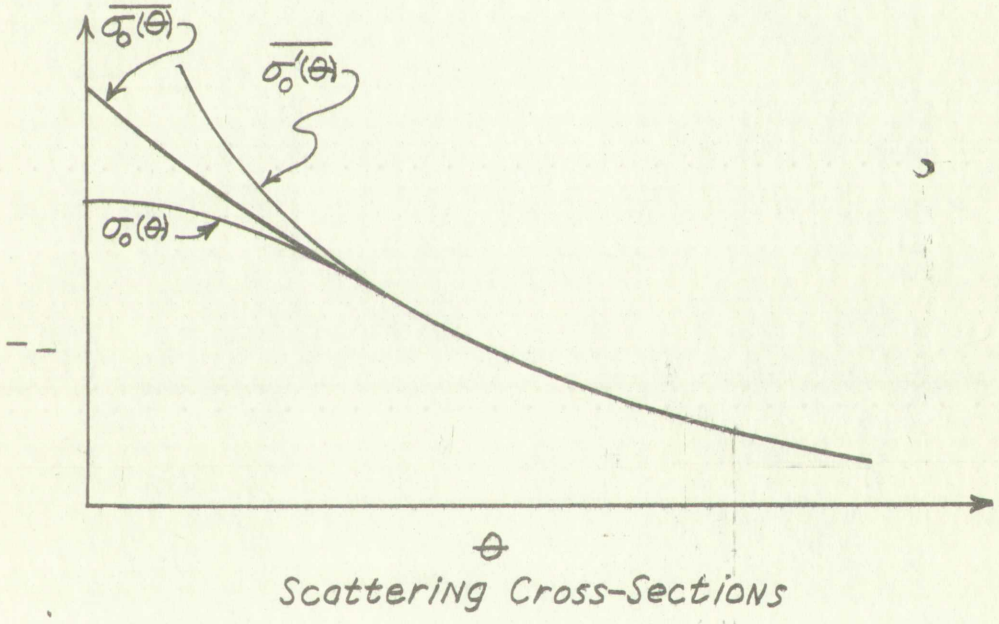

Figure 6

Very recently a different approach to the problem has been examined and the results of the Davies' model have been fitted to some of the experimental data.[9] This method of

[9] A. R. Edison, "Reflection and Scattering Coefficients for Several Types of Targets," UNM Exp. Sta. Tech. Report EE-8 (Sept. 1957).

reducing the Sandia Corporation data is the subject of the next paragraph.

3.3 Theoretical Curve Fitting to Experimental Data. The data taken in the Sandia program would be more useful if theoretical curves for the scattering cross-section could be fitted to the data by adjusting certain parameters.

The theory described in Section 2.2 may be quite valid, but the integral has not been completely evaluated, so it cannot be used to find a family of curves to fit the experimental data for different ground parameters.

Computations of the radar cross-section per unit area for terrain indicate that the scattering cross-section is different than would be obtained with an isotropic scatterer. A theoretical development of this pattern which has been presented by Davies[10] considers a horizontal correlation distance between irregularities and the standard deviation of the vertical fluctuations as the parameters.

The result, which is based on a perfectly conducting rough surface, can be expressed as:

$$\sigma_o(\theta) = \frac{a^2 \sec\theta}{4b^2} \exp\left[\frac{-a^2 \tan^2(\theta)}{2b^2}\right] \qquad (10)$$

---

[10] H. Davies, op. cit. (Ref. 6).

where "a" is the horizontal correlation distance, and "b" is the standard deviation of vertical fluctuations. Note that carrying this into $\theta = 0$, is questionable,[11] but it will be done here since nothing better is available.

This expression compares favorably with experimental results obtained for return from farmland and wooded areas when a suitable loss factor is included to account for absorption in the ground.

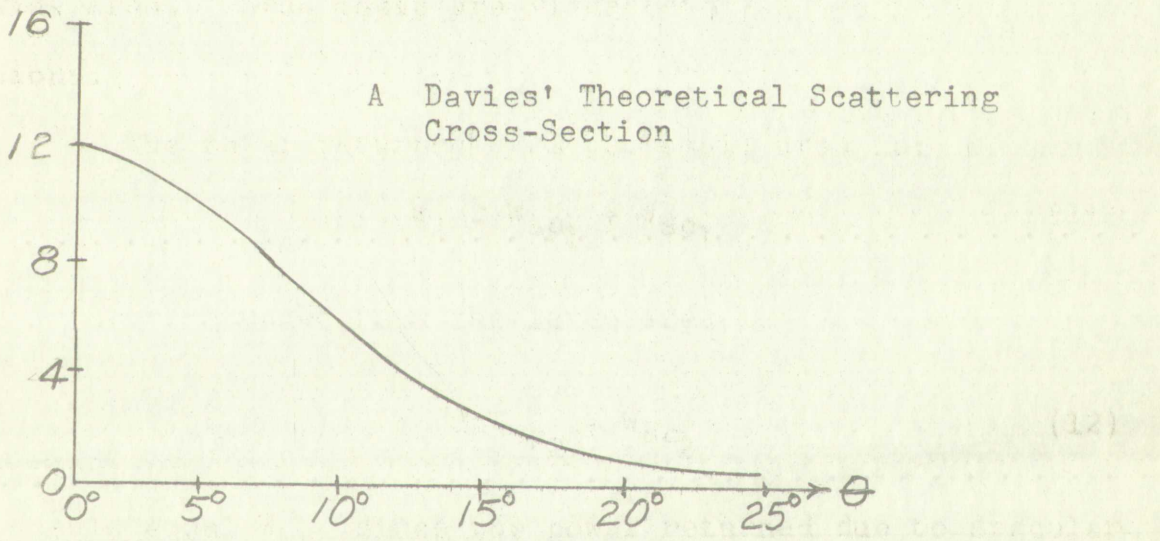

Figure 7

Figure 7 gives one of a family of these curves for a particular ratio of the ground parameters, $a^2/b^2 = 50$. The general shape of the curves for different values of a^2/b^2 is the same, but they tend to become steeper with increasing values of the parameter a^2/b^2.

---

[11] R. K. Moore, op. cit. (Ref. 3).

4.0 Dual Beam Experiment.

Another method of taking data that should lend itself to easier reduction is one in which both a very small area of the ground and a larger area are illuminated. If the small area is small enough so that nearly all the power returned is specular, this power can be subtracted from the power returned from the large area to give the scattered power returned from the wide area. These ideas are illustrated in the following equations.

The power returned from the small area is:

$$W_1 = W_{sp_1} + W_{sc_1} \tag{11}$$

and the power returned from the large area is:

$$W_2 = W_{sp_2} + W_{sc_2} \tag{12}$$

W_{sp_1} should equal W_{sp_2} since the power returned due to specular reflection is independent of illuminated area (assuming the same gain). If the smaller area illuminated is small enough, the scattered power returned will be much less than the specular power and the approximation shown below can be made that:

$$W_1 = W_{sp_1} \tag{13}$$

An approximation to the scattered power returned to the wide beam antenna can then be obtained by subtracting the power returned to the narrow beam antenna from the power returned to the wide beam antenna. The approximation for the

scattered power returned to the wide beam can be used to find the average scattering cross-section.

The idea of illuminating a large and small area so that the specular and scattered power could be separated is due to Dr. Bennett L. Basore.*

There are several methods of illuminating a small and large area on the ground. One method would use a radar pulsed alternately with long and short pulses; however, this method would be difficult because the modulator would have to put out two alternate pulses of different widths. Another method would use a wide-beam antenna and a narrow-beam antenna for alternate runs over the same area, but this method would involve flying over the same area twice which is expensive and difficult. The best method appears to be one that uses two antennas pulsed alternately. One antenna has a broad beam while the other has a quite narrow beam. The two antenna beams allow returned signals to be measured from a large and a small area on the ground. The equations for the return to each antenna due to both scattering and reflection are listed below and will be examined more thoroughly.

4.1 Theory of the Dual-Beam Experiment. The return to each antenna would be the sum of the specular and scattered

* Formerly with Sandia Corporation.

power as given in (7). The only difference in the two expressions for the return will be the different gain factors for each antenna.

The return to the narrow antenna is:

$$\overline{P_{r_1}(t)} = \frac{P_{t_1}(t-\frac{2h}{c})G_1^2(0)\lambda^2K^2}{64\pi^2h^2} + \frac{\lambda^2}{32\pi^2}\int_{r_1}^{r_2}\frac{P_{t_1}(t-\frac{2r}{c})G_1^2(\theta)\sigma_0(\theta)\,dr}{r^3} \qquad (14)$$

and the return to the wide beam antenna would be:

$$\overline{P_{r_2}(t)} = \frac{P_{t_2}(t-\frac{2h}{c})G_2^2(0)\lambda^2K^2}{64\pi^2h^2} + \frac{\lambda^2}{32\pi^2}\int_{r_1}^{r_2}\frac{P_{t_2}(t-\frac{2r}{c})G_2^2(\theta)\sigma_0(\theta)\,dr}{r^3} \qquad (15)$$

The integral in (14) is assumed to be much less than the first term (if the antenna beam is narrow enough) so that it may be dropped out and (14) becomes:

$$\overline{P_{r_1}(t)} \approx \frac{P_{t_1}(t-\frac{2h}{c})G_1^2(0)\lambda^2K^2}{64\pi^2h^2} \qquad (16)$$

If

$$P_{t_1}(t-\tfrac{2h}{c})G_1^2(0) = P_{t_2}(t-\tfrac{2h}{c})G_2^2(0), \qquad (17)$$

the value of (16) will be equal to the first term in (15), and (14) may than be subtracted from (15) to give the power returned from the ground due to scattering to the wide beam antenna. With the specular power removed from the total return, the values of $\overline{\sigma_o(\theta)}$ should vary much less than those in Figure 6, and they should approximate $\sigma_o(\theta)$ much closer since the δ function that was averaged with $\sigma_o(\theta)$ to give $\overline{\sigma_o'(\theta)}$ has been removed. Thus

$$\overline{\sigma_o(\theta)} = \frac{\overline{P_{r_2}(t)}}{\frac{\lambda^2}{32\pi^2}\int_{r_1}^{r_2}\frac{P_{t_2}^2(t-\frac{2r}{c})G^2(\theta)dr}{r^3}} \qquad (18)$$

This appears to be the best method found to date of collecting near-vertical radar return data. There will be a small error in assuming that the return to the narrow antenna is all specular. This error is discussed more fully in Section 7.2 and some examples are calculated to illustrate its magnitude.

Before proceeding to the next section note that the equality stated in (17) and used in (18) implies not only that the magnitudes must be equal, but also that the pulse shapes must be identical.

Figure 8 shows Pr_2, the total returned power, as the sum of Pr_{sc_2}, the scattered power returned to the wide beam antenna and Pr_{sp_2}, the specular power returned to the wide beam

antenna. Pr_{sp_2} is approximately Pr_1, the total power returned to the narrow beam antenna as discussed in the theory of the dual beam experiment. To separate Pr_{sp_2} when Pr_{sc_2} and Pr_2 are known, Pr_{sc_2} is subtracted point by point from Pr_2. Actually, these pulses are average pulses, as discussed in 2.12.

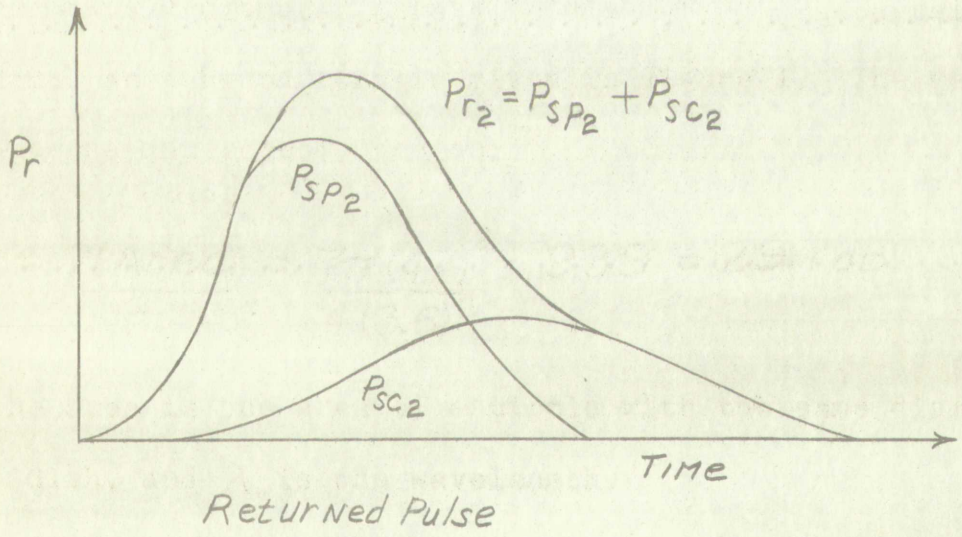

Figure 8

4.2 System Parameters. Section 4.1 has developed the theory for the dual beam experiment, but the parameters given in the equations must be chosen so that the data will have maximum significance. These parameters are given in the next sections

with the reasons for the selection of the values for each parameter.

4.21 Antennas. The narrow-beam antenna should illuminate only a very small area beneath the radar so that the return to it will be almost all specular. The scattered power returned due to scattering is a function of the beam width of the antenna, as shown in (6). Rough calculations indicate that the beam width of the narrow-beam antenna should be less than 10° at the half-power points to keep the scattered power at a minimum.

A 47" diameter parabolic dish at NRL meets this requirement, and the pattern is given in Figure 1. The gain of this antenna can be computed as:[12]

$$G_o = \frac{7(\text{Area})}{\lambda^2} = \frac{7\pi(47)^2}{4(3.6)^2} = 939 = 29.7db \qquad (19)$$

Here the area is the area of a circle with the same diameter at the dish, and λ is the wavelength.

The wide beam width necessary can be obtained with a horn antenna of small dimensions, which is convenient since only a small amount of room is available to mount the horn concentrically with the parabola. A suitable horn has not yet been

---

[12] Reference Data for Radio Engineers, Int. Tel. and Tel. Company, p. 700 4th Edition, 67 Broad St., N.Y. 4, N.Y. (1956).

constructed so nothing but an empirical expression can be used for the gain and pattern.

The gain of the antenna at a point on the axis is given by:

$$G_0 = \frac{10AB}{\lambda^2} = \frac{10(5)(4)}{(3.6)^2} = 15.43 = 11.9 db. \qquad (20)$$

where A and B are the aperture dimensions (5" and 4") and λ is the wavelength.[13] The dimensions of the aperture of the horn were chosen because a horn of this size will fit in the parabola and because these dimensions give a beam width between the half-power points of about 50° in the E and H plane. With this beam width enough scattered power is returned to determine the scattering cross-section over a significant range of angles.

A useful approximation for a horn antenna is $G_0 \cos^2 n\theta$, where G_0 is the gain on the axis and n is a factor that will give the desired beam width at the half-power points. The value n to give a 50° beam width is 1.8 which gives an antenna gain of:

$$G = 15.4 \cos^2 1.8\theta \qquad (21)$$

---

[13] Reference Data for Radio Engineers, op. cit. p. 698 (Ref. 11).

This approximation can be checked roughly with curves given by Silver.[14]

4.22 Transmitted Frequency. It has been shown[15] that "S" band is about the highest frequency for which appreciable amounts of specular power are likely to be returned. For this reason the experiment should be conducted at this or a lower frequency. "X" band would be a very convenient frequency to work with because all of the components are smaller than those for "S" band. However, the fluctuations of the ground levels are ordinarily so large compared with a wavelength at "X" band that no appreciable specular power is returned.

"S" band equipment available at NRL has a frequency of 3280 mc which is near enough to the frequency used by Sandia Corporation to compare results.

4.23 Pulse Width. In the reduction of the data for the average scattering cross-section, the limits on the integral are determined by the pulse width. The range of the limits on the integral, in turn, determine the range of values of θ over which the values of the scattering cross-section are determined. It

---

[14]Samuel Silver Editor, Microwave Antenna Theory and Design, Radiation Laboratory Series (McGraw-Hill Book Co., New York, 1949) pp. 359, 360.

[15]R. K. Moore, op. cit. (Ref. 3).

would be desirable to use as narrow a pulse as possible so that the values of the average scattering cross-section reduced from the data would more nearly approach the actual values of the scattering cross-section. The narrowest pulse which can be generated by the NRL equipment is 1/4 μsec. This, although not as narrow as desirable, should be adequate to give values of $\overline{\sigma_o(\theta)}$ that can be fitted with a theoretical curve. The shape of the pulse is shown in Figure 1.

4.24 Pulse Shape Distortion. The overall bandwidth of the receiver that NRL will use in the dual-beam experiment is 5 mc. This value of bandwidth will cause some distortion of each returned pulse depending on the returned pulse itself.[16]

If the receiver is divided into two components, the first consisting of the R.F. Network and the second consisting of the Amplifier-Detector, it can be shown that the transmitted pulse passed through the R.F. network can be used as the transmitted pulse with no correction to the returned pulses needed. The transmitted pulse passed through the R.F. network is defined as P*.[17]

---

[16] R. A. Hessemer, Jr., and C. S. Williams, Jr., "Determination of Radar Cross-Section For a Scattering Ground," Sandia Corp. Tech. Memo. 206-54-54. (Sept. 1954).

[17] R. A. Hessemer, Jr., and C. S. Williams, Jr., (Ref. 16).

P* can also be found by convolving the transmitted pulse with the low pass equivalent to the transfer function of the receiver.[18]

To prove the statements made above concerning the use of P_1^* the assumption that any non-linear element (such as the R.F. network) must be followed by an element of infinite bandwidth (such as the Amplifier-Detector) is necessary.[19]

4.25 Peak Transmitted Pulse Power. The receiver at NRL has a dynamic linear range of 8 to 120μv into 50 ohms which gives a range of 1.28 to 298$\mu\mu$w with linear I.F. strips. The range in power over the linear portion of the NRL receiver is 23.5 db starting at the point in the receiver characteristic where the signal is equal to the noise. The return for any pulse is assumed to be composed of many phasors of uniform length with a uniform distribution of phases between 0 and 2π radians, which is the random walk problem in two dimensions which gives a Raleigh distribution with a range of fading between the 5 percentile values of 18 db.[20] Using the portion of the linear range between 16μv and 120μv gives a range of signal power of only 17.5 db

---

[18] Janza, Hessemer, and Williams "Pulse Response of Terrain Return Program Receivers", Sandia Corp. Tech. Memo 208-54-54.

[19] R. A. Hessemer, Jr., and C. S. Williams, Jr., op. cit. (Ref. 15).

[20] R. K. Moore, op. cit. (Ref. 1)

which is not enough dynamic range to accurately take data, and the problems of setting the transmitted power so that the returned signals fell in the linear range of the receiver would be quite difficult.

Above the linear portion of the response curve of the receiver is an additional 5 db of range which is non-linear. This section of the response curve can also be used if the Amplifier-Detector has a bandwidth greater than that in the IF strips. This is generally the case so no assumption made in Section 4.24 is invalidated.

A median input of 72$\mu\mu$watts (or 60μv) will give a range of 11.5 db from 16 to 60μv and 6 db from 60 to 120μv which should, with the additional 5 db of non-linear gain of the IF's, be enough dynamic range to gather useful data. Also, the transmitted power will not have to be set exactly to obtain data with the input near 72$\mu\mu$watts. The transmitted power with this input should be 1.8, 3.5, 40.5 watts for 4,000', 7,000' and 12,000' respectively. These calculations are made by dividing the product of the peak returned power (for 1 watt transmitted) given in Figures 13, 14 and 15 and the antenna gain squared into the median power desired at the receiver.

5.0 Experiment Design.

The parameters of the equations for the return to the two antennas, (14) and (15), have been determined except for

the altitude, targets, PRF and the recording equipment which must be selected in terms of the equipment NRL has on hand and of collecting data that is representative of many targets. These items will be selected with these two viewpoints in mind.

5.1 Targets. The targets over which data are taken should be quite varied, with the actual targets selected according to the type of target for which data are desired. However, it would be of some help in the interpretation and comparison of the data if the flights were made over some of the same targets used in the Sandia Corporation experiments. These targets are listed in Table II by type and the time of year of the flight, with the conditions of the target also given. A detailed description of each target can be obtained from Sandia Corporation so that flights may be made over the exact targets used.[21]

Since the targets used by Sandia Corporation are all over a few hundred miles from Washington, D. C., an airbase near each one should be used as a base of operations. On the flights to these points of operation there would be no reason why data could not be taken for short intervals over some of the cities and farmland in the flight path of the R5D. This would gather more data per hour of operation of the aircraft and give much more total data.

---

[21] See Appendix I.

Table II

SANDIA CORPORATION TARGETS

No.	Type	Location	Season	Snow
1.	Commercial, Apartment area	K. C.		
1a.		K. C.	Summer	
2.	Farms with woods and fields	Osborne, Mo.	Winter	
2a.		Osborne, Mo.	Summer	
3.	Same as 2, with railroad	Cameron, Mo.	Winter	Light Patches
3a.		Cameron, Mo.	Summer	
4.	Fields	Sioux City, Iowa	Winter	8" deep, 25%
4a.		Sioux City, Iowa	Summer	
5.	Irrigated fields and orchard	Las Cruces, N.M.	Sept.	
5a.		Las Cruces, N.M.	Nov.	
6.	Dry desert, some vegetation	Albuquerque, N.M.	Fall	
7.	Lake, small ripples	Elephant Butte, N. M.	Sept.	
7a.		Elephant Butte, N. M.	Jan.	
8.	Dry desert, arroyo, highway	Near Salton Sea, Calif.	Fall	
8a.		Near Salton Sea, Calif.	Winter	
9.	Ocean, swells, sea state	Near Long Beach, Calif.		
9a.		Santa Ana - Santa Cruz Islands, California		
10.	Orchard	El Toro, Calif.	Fall	
11.	Lake, small waves	Salton Sea, Calif.		
11a.	Smooth Lake	Salton Sea, Calif.		
12.	Rangeland	Magdalena, N.M.	Winter	3 or 4" deep, dry
13.	Fields	Breckenridge, Minn.	Winter	8" deep, dry
13a.		Breckenridge, Minn.	Summer	
14.	Lake, frozen	Bemidji, Minn.	Winter	10" deep, dry

No.	Type	Location	Season	Snow
14a.	Lake, Small waves	Bemidji, Minn.	Summer	
15.	Fields and woods	Bemidji, Minn.	Winter	10" deep, dry
15a.		Bemidji, Minn.	Summer	
16.	Lake, heavy ripples	Caballo, N. M.	Winter	
17.	Dry desert, abandoned runways	Belen, N.M.		
18.	Lake, frozen	Alexandria, Minn.		
19.	Salt flats	Salt Lake		
20.	Forest	Pine Island, Minn.	Summer	
20a.		Pine Island, Minn.	Winter	12-18", dry
21.	Commercial area	Minneapolis, Minn.	Summer	
21a.		Minneapolis, Minn.	Winter	5"
22.	Residential area	Minneapolis, Minn.	Summer	
22a.		Minneapolis, Minn.	Winter	7"
23.	Airfield Runways	Albuquerque, N.M.	Summer	
24.	Irrigated fields with vegetation	Imperial Valley, Calif.	Winter	
25.	Airfield runway	El Centro, Calif.	Winter	
26.	Sandy desert	Muroc Target No. 1	Winter	Wet Under
27.	Sand hills	Near Muroc Lake	Winter	
28.	Lake, waves	Lake Mead, Calif.		
29.	Dry Salt Lake	Yucca Lake Target	Winter	Wet Under
30.	Sand Hills	1 Mi. No. of Yucca Lake	Winter	
31.	Desert II	Near Salton Sea	Winter	
32.	Residential	Santa Ana, Calif.	Summer	
33.	Residential	Presque Isle, Me.	Winter	20"-25"
34.	Residential	Superior, Wis.	Winter	10"-12"
35.	Forest	S. of Presque Isle	Winter	20"-25"
36.	Airfield	Loring AFB	Winter	20"-25"
37.	Snowfield	NE of Presque Isle	Winter	20"-25"

5.2 Altitudes. The altitudes, particularly over the targets used by Sandia Corporation should be 4,000, 7,000 and 12,000 feet, or any combination if more than one altitude can be used. If only one altitude can be used, it should be approximately 7,000 feet or higher above the terrain. Data taken by Sandia Corporation has fewer unexplainable deviations at these altitudes; that is, the curves of $\sigma_0(\theta)$ do not vary erratically with θ. Sandia Corporation data for these altitudes would make the comparison between NRL data and Sandia data easier.

5.3 Recording Equipment. The returned pulses will be displayed on an "A" scope and recorded by explosing each frame of film with 75 to 100 pulses. This should be adequate to give a good mean pulse shape for the return from the ground for the pulses recorded. The mean will either be read from the film with the use of a microdensitometer or by determining visually what appears to be the average returned pulse.

A check on the peak of the mean value could also be obtained by recording only the peaks, as the Wave Propagation Branch at NRL has been doing in pulse-to-pulse sea return data. This has the advantage that data taken in this manner can be reduced by machine methods and may be more accurate in determining the peak of the mean than the multi-exposed film. This method could not be used to record the peak while the multi-exposed film could be used to gather only the shape of the average returned pulse.

If possible, some record should be made of the terrain from which data is gathered. This can be accomplished by taking aerial photographs of the ground at a rate that will give some overlapping of the different exposures. These photographs should be synchronized with the oscilloscope camera so that correlation is possible.

5.4 Antenna Mounting. It is proposed that the two antennas be mounted concentrically so that there will be no errors due to looking at slightly different terrain due to different physical locations on the R5D or due to small errors in the servo systems that operate the antenna mounts. Actually if the antennas were mounted in different pods on the same wing, the error would not be noticeable as far as angular resolution is concerned. If the antennas were mounted 100 feet apart, this would given an error of 1.5 degrees at 4,000 feet which would make very little difference in the variation of the reduced scattering coefficients with angle of incidence. However, a separation of 100 feet between transmitting and receiving antennas might be enough to affect the amount of specular power received by the antennas. The planned antennas are shown in a side view.

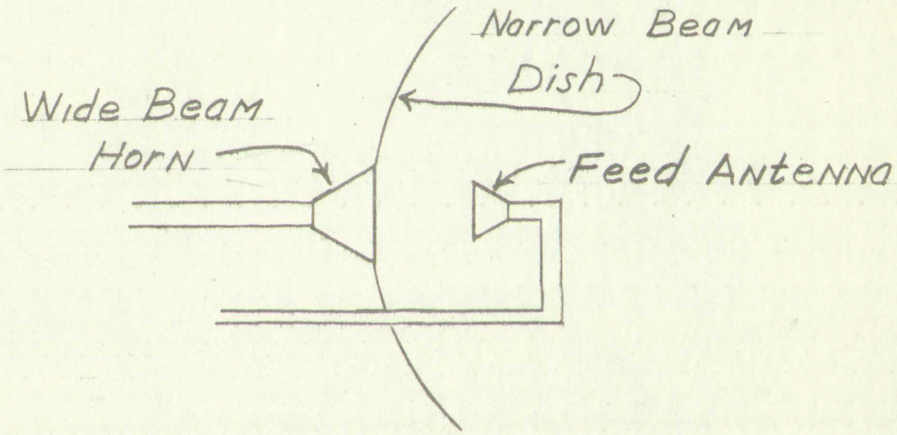

Physical Arrangement of The Antennas

Figure 9

One feed should have a slow 90° turn so that the two antennas are polarized at right angles to each other. Shorting bars across the opening of each horn to short out the polarization of the other antenna should give good isolation between the antennas. Isolation will insure that no power leaks back through the other antenna and ferrite switch to be retransmitted with time delay or the other gain.

It will be necessary, of course, to take antenna pattern measurements after the antennas are assembled in order to get the effect of this configuration on the patterns of each antenna.

5.5 Ferrite Switch. It will be desirable to collect data from both antennas over almost the same terrain so that the parameters that describe the ground will be the same for the power returned to both antennas. The easiest method to gather data in this manner would be to use a ferrite switch to pulse the antennas alternately because it would allow a higher switching rate than a mechanical switch.

If a ferrite switch is not used, a mechanical method that might alternate between antennas at about 50 cps could be used.

5.6 Block Diagram. A possible block diagram is given in Figure 3, which gives only a portion of the components used. The block diagram is a combination of the requirements of the

experiment and the one Sandia Corporation used. A few comments on operation and components of the system are given below.

The transmitted pulse is propagated by either the narrow beam or wide beam antenna, depending on which antenna is switched in by the ferrite switch. The received pulse is returned by the same antenna which is coupled to the receiver which contains the components from the R.F. amplifiers through the detector. The output of the receiver is coupled to two oscilloscopes to record the received pulses.

The system trigger is used to synchronize the whole system, to trigger the marker generator and to provide a delayed trigger (through the delay circuit) to the scopes to provide an expanded display of the returned pulse.

The signal generator is used to provide a power reference, and, by inserting it into the receiver, a measure of receiver stability can be obtained by the fluctuations, or lack of fluctuations of this pulse.

5.7 Sampling Rate and Size of Samples. One of the most important considerations concerns the sampling rate (or PRF) since a biased estimate of the average return would result if too few independent samples were taken. To determine what the

sampling rate should be for independent samples, one may consider that a CW signal is being transmitted which, when detected, has amplitude fading due to the manner in which the phasors add up at the antenna, but which is never negative due to detection. Such a time series is shown below

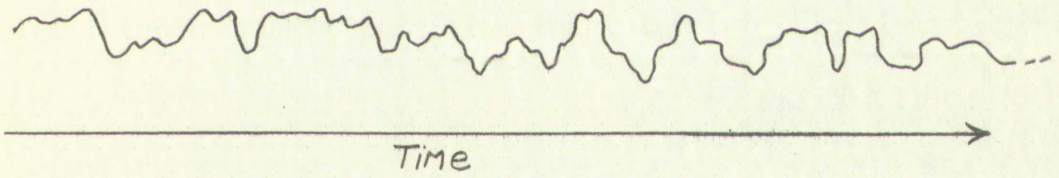

Figure 10

The effect of transmitting pulses is as if one used periodic "gates" to "sample" the continuous time series. The rate of sampling could be determined by finding $\phi(\gamma)$, the autocorrelation function, for this series since the autocorrelation function gives a measure of the statistical dependency between points in the time series as a function of their separation. From the autocorrelation function it is possible to pick a value of the time between samples so that the dependence between samples

is very small. This, then, should be the separation between the pulses that are sampling the time series in Figure 10, since only first order statistics will be obtained.

The time series is not easy to calculate but it can be shown that the Fourier cosine transform of the power spectrum gives the autocorrelation function.[22] The time series of the return is seen through a square law detector, so that instead of a power spectrum of the input voltage, a power spectrum of the detected voltage will be observed. This is here called variance spectrum[23] and its Fourier cosine transform will give the auto-correlation function of the detected signal.[24]

With this function, a separation of time, t, can be chosen so that the correlation between points will be zero, or very small, as mentioned earlier. The calculation of the auto-correlation function by this method indicates that the radar

---

[22]S. O. Rice, "Mathematical Analysis of Random Noise," BSTJ, Vol. 23, p. 312 (1944).

[23]Peter D. Welch, "Progress Report on Intrepretation and Prediction of Radar Terrain Return Fading Spectra," Physical Science Laboratory Report AER-14W, New Mexico A. & M. A., College Station, New Mexico

[24]S. O. Rice "Mathematical Analysis of Random Noise," BSTJ, Vol. 24, pp. 125-126 (1945).

should have a prf of 100 to 200 pulses per second or less for all pulse amplitudes to be independent.

.5.8 Aircraft Speed. The speed of the R5D should be around 150 knots. This is a safe cruising speed and it is not so fast that any significant distance is covered between pulses.

6.0 Calibrations.

The success of this experiment, as of any other (particularly at microwave frequencies), depends on the accuracy of the calibrations. The larger errors will probably be in the measurements of the transmitted power, received power, and the antenna patterns.

A method of measuring these parameters is suggested along with a discussion of the accuracy needed, but the actual details will be left to the NRL personnel conducting the experiment, due to their extensive experience in this field.

The procedure that NRL uses measures the ratio of transmitted power to received power. This ratio is all that is necessary to find the scattering cross-sections as given by (18), but for the data reduction in this experiment the ratio of the transmitted power to both the narrow- and the wide-beam return will be needed. The subtraction of the narrow-beam ratio from the wide-beam ratio will give the ratio necessary for the reduction of the data by (18). These will actually be ratios of attenuator settings as discussed in the following paragraphs.

6.1 Calibration of Transmitted and Received Power.

The calibration procedure uses the arrangement of the equipment shown in Figure 11,

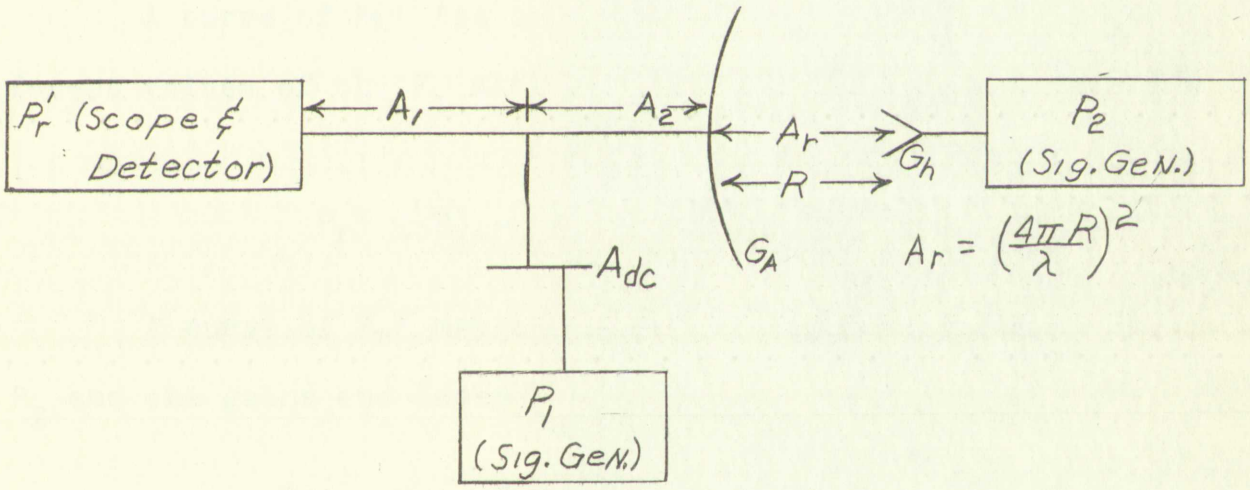

Equipment Used For Calibrations

Figure 11

where all quantities are in decibels and

P_1 = Attenuator setting of internal signal generator

P_2 = Attenuator setting of external signal generator

$P_{r'}$ = Received power at the receiver

A_{dc} = Loss in directional coupler

A_1 = Line loss from directional coupler to receiver

A_2 = Line loss from directional coupler to antenna

A_r = Attenuation of signal through the known distance; R

G_h = Gain of standard antenna

G_a = Gain of radar antenna

The calibration procedure given below will allow the power returned to be calibrated in terms of a signal generator. The procedure and expressions relating the system parameters are given below.

A curve of P_r' (as scope deflections) is first made for different values of the P_1 attenuation which gives:

$$P_r' = P_1 - A_{dc} - A_1 \qquad (22)$$

A curve of P_r' may also be made in terms of settings of P_2 and the gains and losses P_2 undergoes to give:

$$P_r' = P_2 + G_h - A_r + G_a - A_2 - A_1 \qquad (23)$$

where P_2 can be determined in watts with the aid of a power bridge. These two expressions for P_r' (22 and 23) can be equated and rearranged to give:

$$P_1 = (P_2 + G_h - A_r) + A_{dc} + G_a - A_2 \qquad (24)$$

However, the quantity in parenthesis in (24) is P_r, the power received by the antenna, resulting in:

$$P_r = P_1 - Ad_c - G_a + A_2 \qquad (25)$$

A curve of P_2 versus P_1 can be obtained from the curves of Pr' versus P_1 and P_2, and from (25) a curve of P_r versus P_1 can be made. Thus, to calibrate the peak of a returned pulse, one finds what value of P_1 this peak power corresponds to from the plot of P_r versus P_1 and this value of P_1 can be related to P_2 through the curve of P_2 versus P_1 to give a check on inflight calibrations with ground calibrations.

The curve of deflection versus Pr, or corresponding values of P_1, that results from this procedure can be used in flight to compare the deflection on the oscilloscope produced by different settings of P_1 with the deflections obtained on the ground. Thus, a factor to correct for changes in receiver performance can be obtained.

The transmitted pulse can be attenuated and inserted into the directional coupler instead of P_1 to give a curve of P_r' versus P_r as given by (26).

$$P_r' = P_t - A_t - A_{dc} - A_1 \qquad (26)$$

where A_t is the attenuation of the transmitted pulse necessary to keep it in the range of the detector and scope.

For any deflection, P_{rn}' the following relationship will be true:

$$P_t - A_t - A_{dc} - A_1 = P_1 - A_{dc} - A_1 \qquad (27)$$

$$\text{Or } P_t = P_1 - A_t \qquad (28)$$

The value of P_1 needed to produce the deflection P_{rn}' is related to P_2 through (24) and P_t is related to P_2 by:

$$P_t = P_2 + G_h - Ar + A_{dc} + G_a - A_2 - A_t \qquad (29)$$

Pr is related to P_2 by:

$$P_r = P_2 + G_h - A_r \qquad (30)$$

and the ratio of P_r to P_t is given by:

$$\frac{\text{Log } P_r}{\text{Log } P_t} = \frac{(P_2 - G_h - A_r)}{(P_2 - G_h - A_r + A_{dc} + G_a - A_2 - A_t)} \qquad (31)$$

Thus the calibration of the ratio P_r/P_t has been found without the necessity of finding the actual amount of power transmitted or received in the R5D.

6.2 Calibrations of Waveguides and Attenuators. Unfortunately, power and attenuation measurements at the frequency to be used in this experiment are not very accurate. Accuracies of under 20 percent are considered excellent while measurements with errors greater than 20 percent are often used as though these measurements were correct to less than 10 percent accuracy. To avoid large errors in the measurements of the returned power, the attenuation given for the microwave components must be checked to

ascertain if the manufacturers' data are correct.

6.3 Antenna Patterns. The equations for the return are developed with the use of the coordinates of a right-hand spherical coordinate system (r, θ, ϕ, see Figure 1). Therefore, to reduce the data, it is necessary to have the antenna patterns as functions of θ and ϕ, as shown in (7). Thus the patterns of the gain as a function of θ for constant ϕ (as shown in Figure 12) should be known. If the pattern has circular symmetry with respect to the Z axis (Figure 4) the integration of ϕ in (6) gives a 2π outside the integral; otherwise, a lengthy numerical integration must be performed in the data analysis. The degree of circular symmetry can only be established by taking the patterns shown below for several values of ϕ.

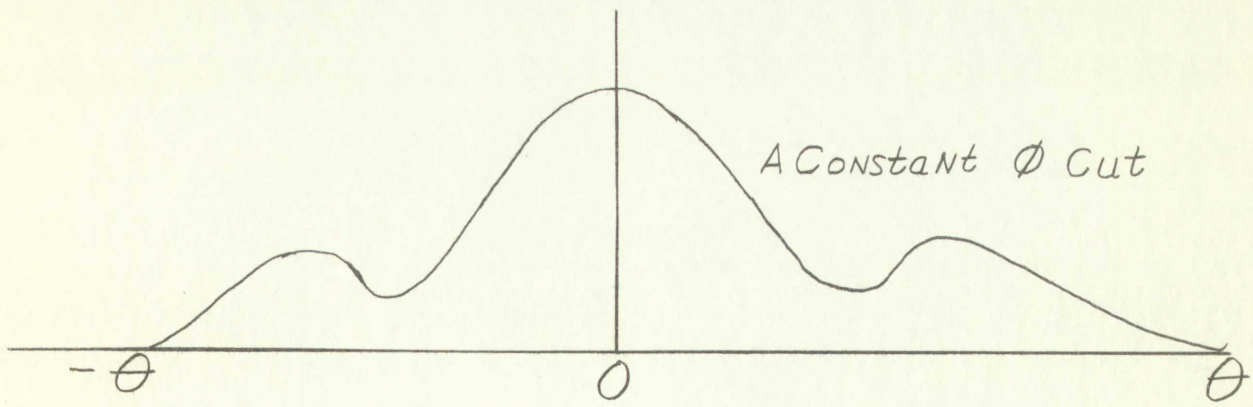

Figure 12

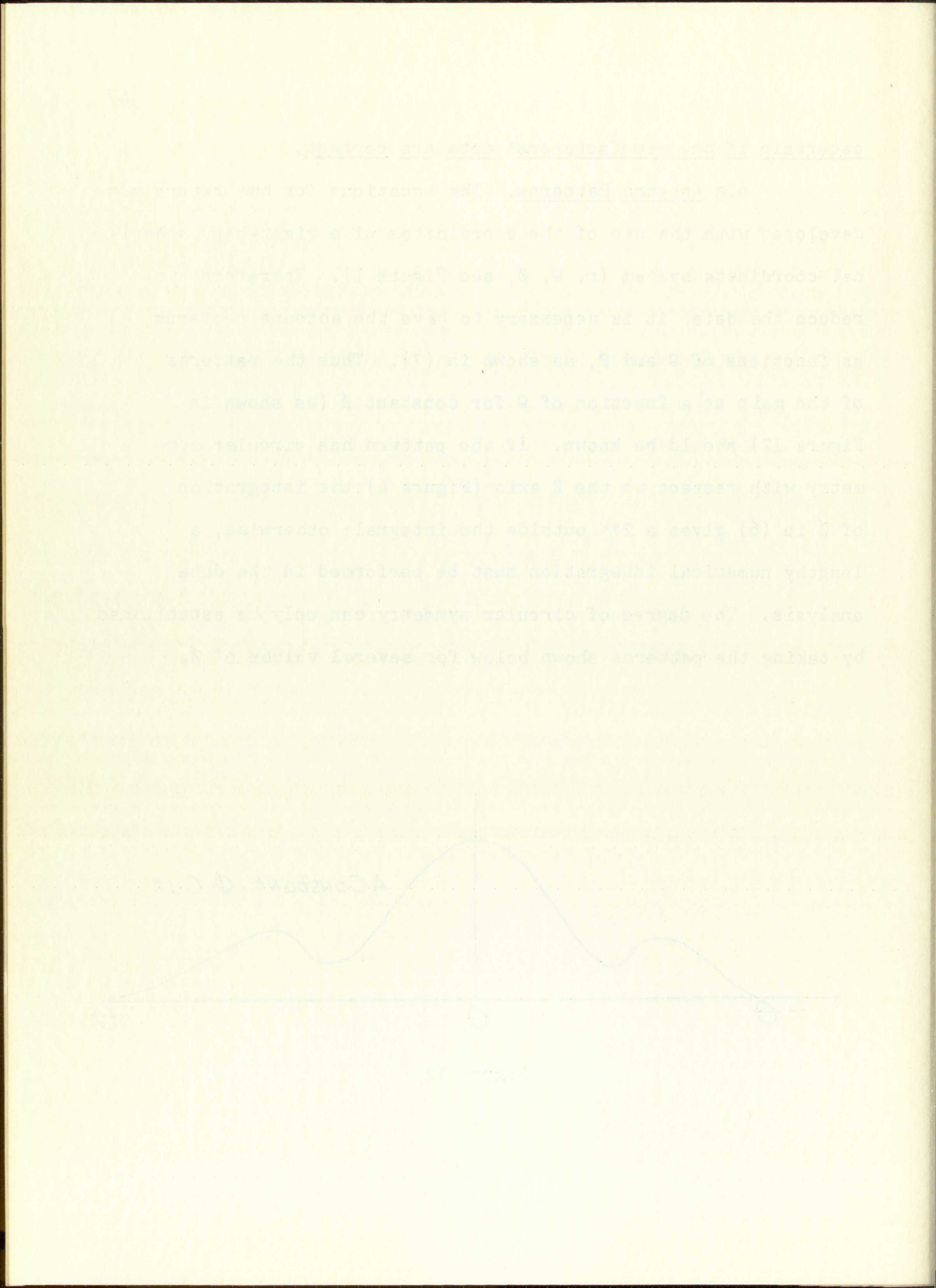

Antenna patterns are frequently taken as functions of azimuthal angles for different elevation angles by the method of great circle cuts. These patterns can then be reduced[25] to patterns in spherical coordinates that can be used in the data reduction.

Most patterns will not be quite symmetrical with respect to the Z axis, but they can often be fitted with an analytical expression for the pattern as a function of θ. Only such a fit weighs all of the different ϕ cuts so that circular symmetry must be assumed. This is a valid approach when the deviation from circular is small.

6.4 Narrow-Beam Attenuator. An attenuator must be placed between the ferrite switch and the narrow-beam antenna so that the gains of the maximum lobes of the antennas will be equal, which will make (16) valid. If (16) is valid, and with the assumption that the power returned to the narrow-beam antenna is almost entirely specular, the power returned to the narrow-beam antenna can be subtracted from the power returned to the wide-beam antenna to give the scattered power returned to the wide-beam antenna.

If the attenuation through the ferrite switch to both antennas is the same the value of this attenuator is the difference (in db) between the gains of the two antennas. This difference will be about 18 db. It might be necessary, however, to leave this attenuator out for a target that has essentially no

[25] J. M. Usry and R. B. Glascock, "Converting Measured Antenna Patterns to Spherical Coordinates," UNM Exp. Sta. Tech. Memo EE-3 (March, 1957).

specular return since the combination of specular and scattered return may be so small as to be almost indiscernible from the noise.

To ascertain whether this is the correct value or not, the R5D can be flown over very smooth water with the antennas pulsed alternately. If the value above is correct, the return from both antennas will be the same. In this determination very little scattered power will be returned to the wide-beam antenna. The relative amount of scattered power returned to the wide-beam antenna will be indicated by the amount of fading in the wide-beam antenna signal. If fading is less than 6 or 8 db, the signal may be considered essentially specular.

7.0 Calculated Results Using Proposed System Parameters.

A few examples of the returned scattered power have been calculated (for one watt transmitted) for one scattering coefficient to show the size of the error in the assumption that the return to the narrow beam is all specular power.

7.1 Calculated Values for the Returned Power. In Figures 13, 14 and 15, the calculated values of the returned power scattered back to the wide-beam antenna have been plotted. The difference in calculated values of the scattered power returned to the narrow-beam antenna and the scattered power returned to the wide-beam antenna have been plotted also as the "net scattered power." The specular power was not included in these

because it would have cancelled.

The scattering cross-section used in the calculations of scattered power is shown in Figure 16. This scattering cross-section is a theoretical curve fitted to data taken over the Pine Island Forest target.[26]

7.2 Scattering Cross-Sections Reduced Using the Dual-Beam Theory. The values for the "net scattered power" returned to the wide-beam antenna have been used to calculate the "scattering cross-sections" to illustrate the error in the dual-beam experiment theory. The scattering cross-sections so calculated (reduced with the aid of (6) are shown in Figure 16, along with the scattering cross-section used in determining the returned powers.

Figure 16, shows that the dual-beam method is satisfactory from the limit of the wide-beam antenna pattern into about the limit of the narrow pattern (5°). This error may be reduced to some degree if the narrow-beam antenna pattern is narrower than the pattern given. The pattern given for the narrow-beam antenna was approximated from E and H plane cuts; if the pattern is narrower between these two planes, the error will be reduced.

8.0 Calculation of Scattering Cross-Sections and Reflection Coefficients for the Dual-Beam Experiment.

The scattering cross-sections can be calculated by

---

[26] A. R. Edison, op. cit. (Ref. 8).

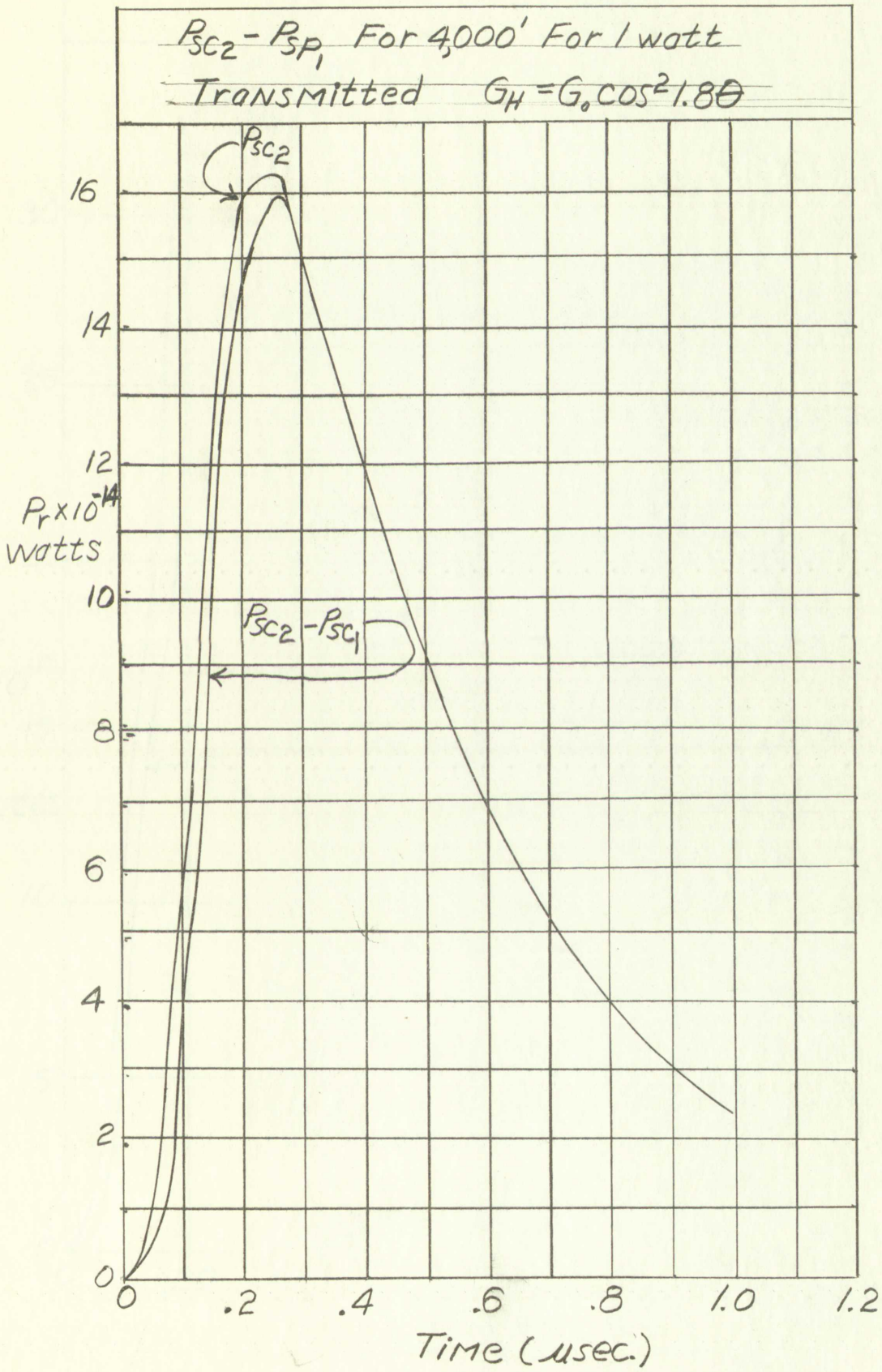
$P_{SC_2} - P_{SP_1}$ For 4,000' For 1 watt
Transmitted $G_H = G_0 \cos^2 1.8\theta$
P_{SC_2}
$P_{SC_2} - P_{SC_1}$
$P_r \times 10^{-14}$ watts
16
14
12
10
8
6
4
2
0
0
.2
.4
.6
.8
1.0
1.2
Time (μsec.)

Figure 13

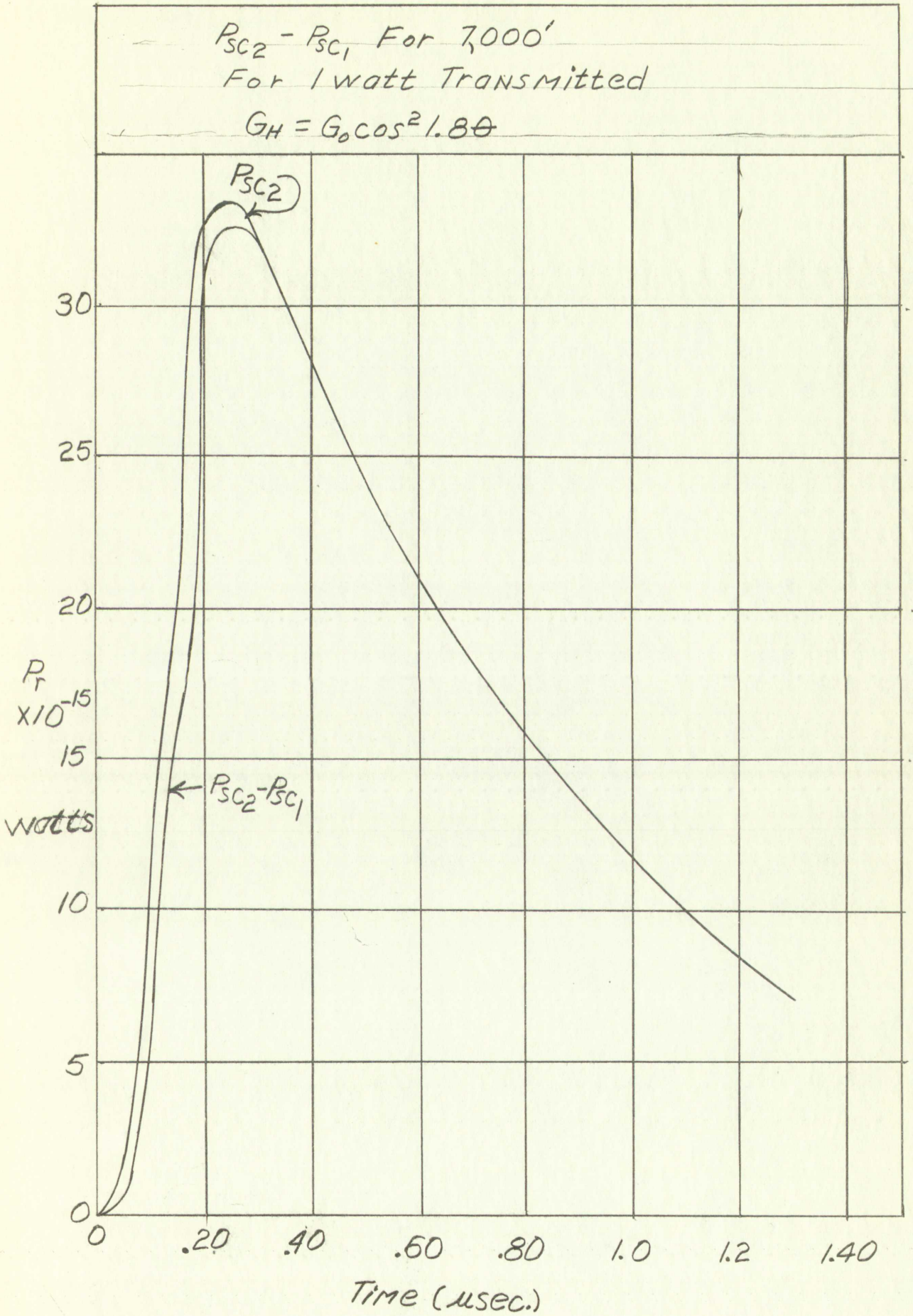
$P_{SC_2} - P_{SC_1}$ For 7,000'
For 1 watt Transmitted
$G_H = G_o \cos^2 1.8\theta$
P_{SC_2}
$P_{SC_2} - P_{SC_1}$
30
25
20
15
10
5
0
P_r $\times 10^{-15}$ watts
0
.20
.40
.60
.80
1.0
1.2
1.40
Time (μsec.)

Figure 14

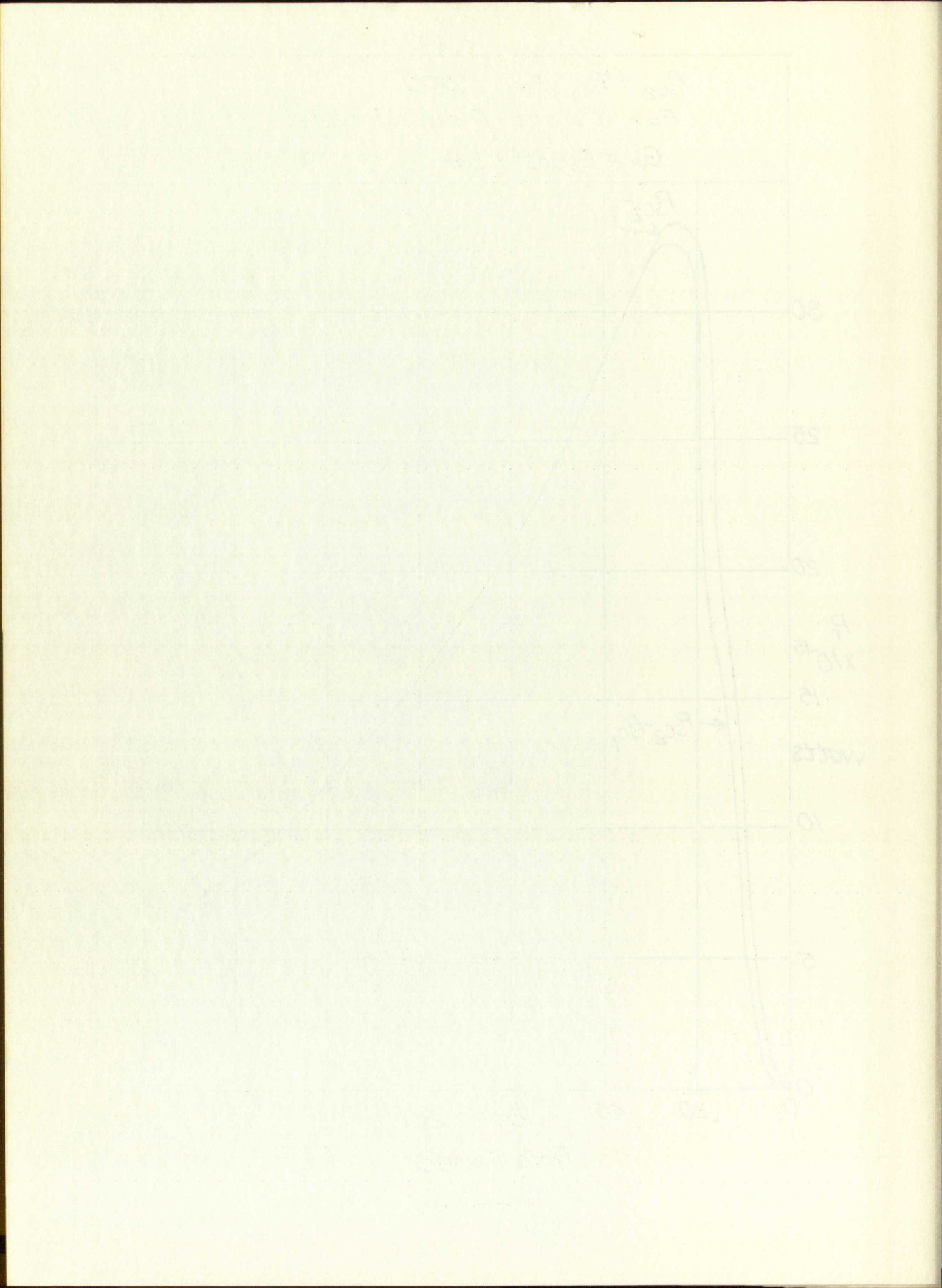

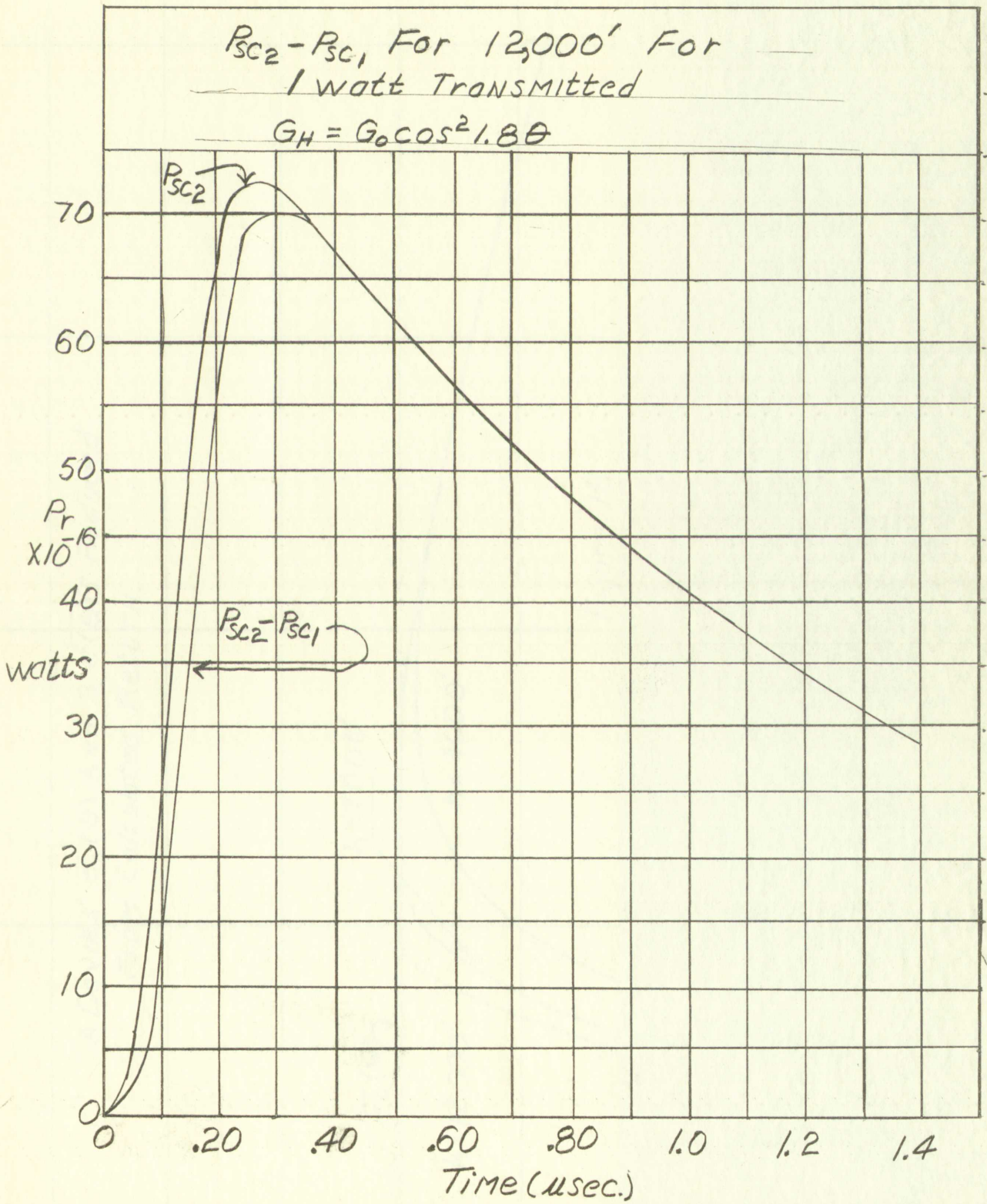
$P_{SC_2} - P_{SC_1}$ For 12,000' For
1 watt Transmitted
$G_H = G_0 \cos^2 1.8\theta$
P_{SC_2}
$P_{SC_2} - P_{SC_1}$
P_r X10^{-16} watts
70
60
50
40
30
20
10
0
0
.20
.40
.60
.80
1.0
1.2
1.4
Time (μsec.)

Figure 15

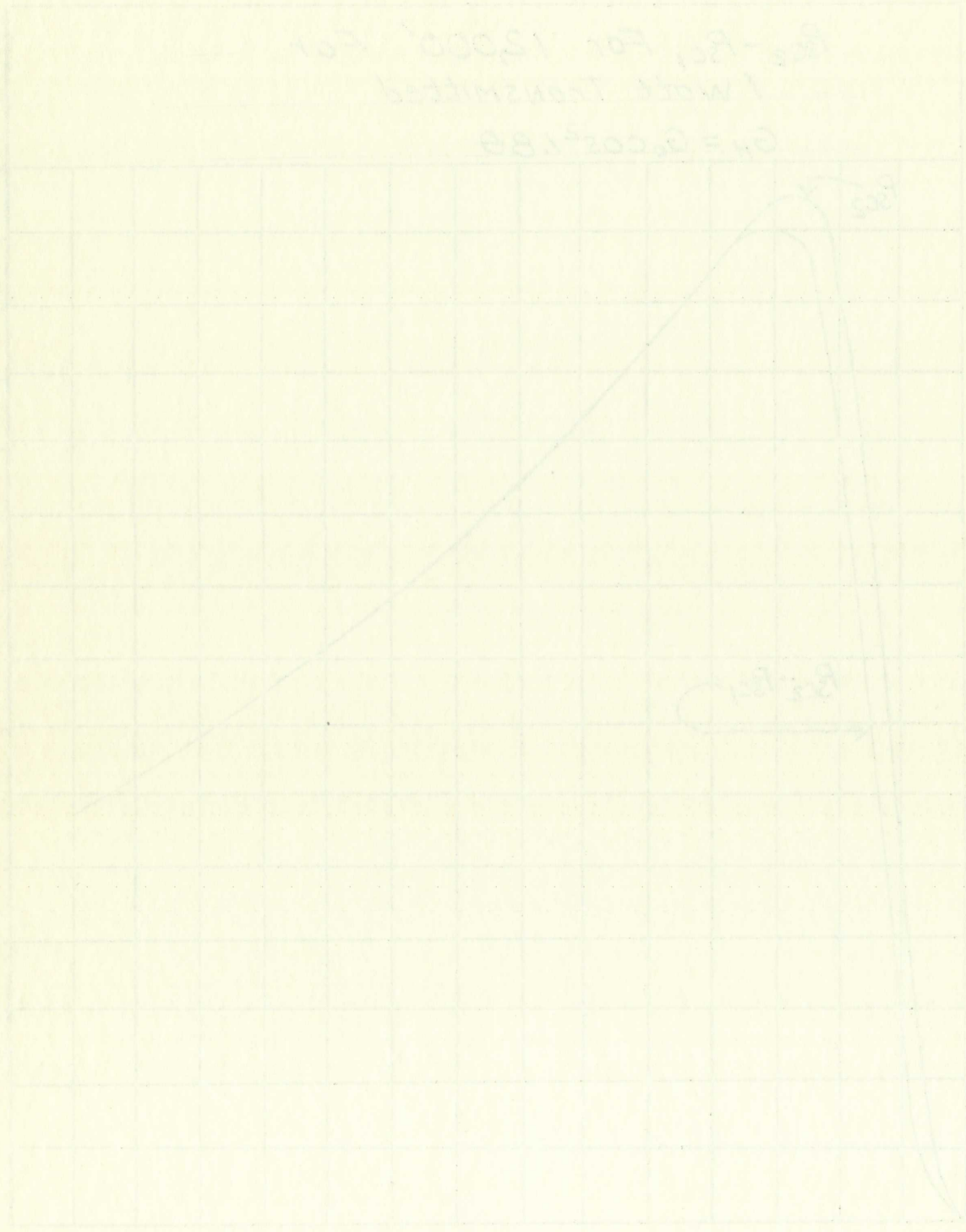

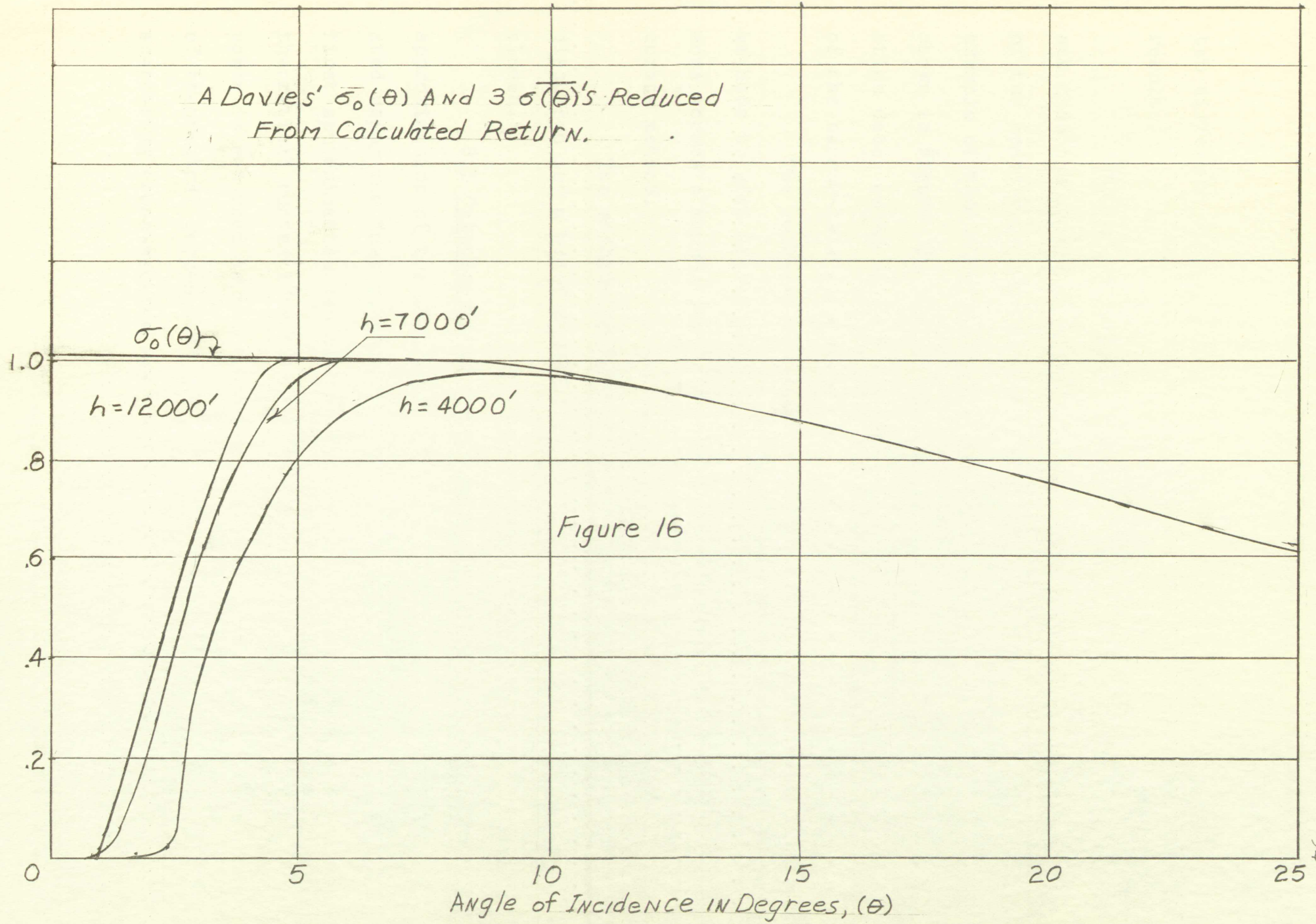
A Davies' $\sigma_0(\theta)$ And 3 $\sigma(\overline{\theta})$'s Reduced From Calculated Return.
$\sigma_0(\theta)$
h=7000'
h=12000'
h=4000'
1.0
.8
.6
.4
.2
0
5
10
15
20
25
Angle of Incidence in Degrees, (θ)

Figure 16

two different methods which will give approximately the same results.

The method of successive approximations is more exact than the method of comparing theoretical curves to the values of the scattering cross-sections reduced from the data. As an example of the latter method the scattering cross-sections shown in Figure 16, which have been reduced from Sandia Corporation data, could be fitted with theoretical curves to the limit of the narrow-beam antenna (5^{o}).

The reflection coefficients may be reduced by two methods to give approximately the same results but, again, the more accurate method requires more computations than the less accurate method.

The methods of calculating these two parameters will be discussed and a brief discussion of plotting the data will be included.

8.1 Calculation of Scattering Cross-Sections. As a first approximation of the scattering cross-section, (18) may be evaluated using the "net scattered power" (as discussed in 7.1). This first approximation can be fitted with several of a family of theoretical curves into the point where appreciable scattered power is returned to the narrow-beam antenna. Any of the family of theoretical curves that fit the first approximation to the scattering cross-section may be satisfactory, depending on the

accuracy desired.

The method of successive approximations can also be used to find $\sigma_o(\theta)$. A value of $\sigma_o(\theta)$ could be assumed and inserted into the equation that results when (14) is subtracted from (15). The correct value of $\sigma_o(\theta)$ will give a calculated value of $P_r(t)$ that will agree with the experimental value.

8.2 Calculation of Reflection Coefficients. As a first approximation to the reflection coefficient, the power returned to the narrow-beam antenna can be used in (1) to calculate the reflection coefficient. A much more accurate method of finding the reflection coefficient is to calculate the scattered power returned to the wide-beam antenna (using the more accurate scattering cross-sections discussed in 8.1), and to subtract it from the total power returned to the wide-beam antenna to find the specular power to use in (1).

The reference cited has[27] substantially reduced the questions concerning the values of θ to use when plotting $\overline{\sigma(\theta)}$ to questions of minor importance. The author gives a theoretical discussion which shows that the position of the peak of the transmitted pulse is the position that should be used in plotting $\overline{\sigma_o(\theta)}$.

---

[27] A. R. Edison, op. cit. (Ref. 8).

8.3 Summary of Data Reduction Procedures. A brief summary of the details and procedures that are to be followed in the reduction of the data will be given here.

On a data run the altitude, transmitted power, frequency and any gain adjustments will be recorded. An inflight calibration should also be made to check with ground calibrations.

After a data run, both the peak return and the multi-exposed films will be read to give the median returned pulse. When the median return pulse is calibrated, the scattering cross-section can be calculated by inserting the correct values for the parameters in (18).

The solution for the scattering cross-section will have to be done by numerical methods which can be done on a desk calculator or digital computer. The solution for the scattering cross-section is a convolution (superposition) integral which is much more difficult to evaluate than an ordinary integral. The solution of this type of integral can be found in the literature.[28]

9.0 Conclusions.

The dual-beam experiment should give better information about the scattering cross-section and reflection

---

[28] Stanford Goldman, Information Theory; (New York, 1955) pp. 223-24.

coefficient of any target than has been available. The calculations that have been made for the proposed system to take the data indicate that the experiment is feasible. However, the restrictions imposed on some of the parameters of the system must be observed rather carefully, particularly in the selection of the narrow-beam antenna. The calculations of the scattering cross-sections (shown in Figure 16) illustrate the effect of the relatively narrow beam used in the calculations.

The data reduced from the experiment will be valid to the angle where the scattered power returned to the narrow beam becomes significant. It should be noted that the data reduced from the dual-beam experiment will be much less susceptible to effects due to specular reflection in the measured scattering cross-sections.

Appendix I

Sandia Corporation Target Description

SCTM-61-55-54, "Target of Terrain Return Project---Site 1, Kansas City, Missouri", D. M. Gragg, April 12, 1955.

SCTM-59-55-54, "Target of Terrain Return Project---Site 2, Farmland Near Osborn, Missouri", D. M. Gragg, April 25, 1955.

SCTM-60-55-54, "Target of Terrain Return Project---Site 6, Wooded Farmland with Railroad Near Cameron, Missouri", D. M. Gragg, May 2, 1955.

SCTM-64-55-54, "Target of Terrain Return Project---Site 8, Flat Farmland Near Sioux City, Iowa, D. M. Gragg, May 3, 1955.

SCTM-226-55-54, "Target of Terrain Return Program---Orchard and Field Near Las Cruces, New Mexico", D. M. Gragg, October 20, 1955.

SCTM-164-55-54, "Target of Terrain Return Project---Dry Mesa West of Albuquerque, New Mexico", D. M. Gragg, August 12, 1955.

SCTM-255-55-54, "Target of Terrain Return Program---Elephant Butte Lake and Caballo Reservoir, New Mexico, D. M. Gragg, October 5, 1955.

SCTM-228-55-54, "Target of Terrain Return Program---Desert Near Salton Sea, Calibornia", D. M. Gragg, October 19, 1955.

SCTM-258-55-54, "Target of Terrain Return Project---Orchard Near El Toro, California, D. M. Gragg, December 7, 1955.

SCTM-254-55-54, "Target of Terrain Retrun Project---Snow-covered Rangeland Northwest of Magdalena, New Mexico, D. M. Gragg, December 6, 1955.

SCTM-62-55-54, "Target of Terrain Return Project---Wahpeton, North Dakota", R. K. Moore, May 3, 1955.

SCTM-163-55-54, "Target of Terrain Return Project---Lake Bemidji, Minnesota", D. M. Gragg, August 2, 1955.

SCTM-162-55-54, "Target of Terrain Return Project---Field Near Woods Near Bemidji, Minnesota", D. M. Gragga, August 1, 1955.

SCTM-266-55-54, "Target of Terrain Return Project---Dry Mesa and Abandoned Runways Near Belen, New Mexico", D. M. Gragg, December 12, 1955.

SCTM-218-54-54, "Target of Terrain Return Project--Pine Island Minnesota", R. K. Moore, September 24, 1954.

SCTM-57-55-54, "Target of Terrain Return Project--Industrial Section, St. Paul, Minnesota", D. M. Gragg, April 6, 1955.

SCTM-58-55-54, "Target of Terrain Return Project---Residential Section, Minneapolis, Minnesota", D. M. Gragg, April 5, 1955.

SCTM-263-55-54, "Target of Terrain Return Project---Yucca Lake, Nevada and Sand Hills North of Yucca Lake", D. M. Gragg, December 8, 1955.

SCTM-8-56-14, "Target of Terrain Return Project--Residential Section Santa Ana, Calif.", D. M. Gragg, January 23, 1956.

SCTM-264-55-54, "Target of Terrain Return Project---Residential Section Presque Isle, Maine, D. M. Gragg, December 9, 1955.

SCTM-267-55-54, "Target of Terrain Return Project---Residential Section Superior, Wisconsin", D. G. Gragg, December 12, 1955.

SCTM-265-55-54, "Target of Terrain Return Project---Forest South of Presque Isle, Maine", D. M. Gragg, December 9, 1955.

SCTM-9-56-14, "Target of Terrain Return Project---Snowfield S. E. of Presque Isle, Maine", D. M. Gragg, January 23, 1956.

BIBLIOGRAPHY

R. K. Moore and C. S. Williams, Jr., "Radar Return at Near Vertical Incidence" Proc IRE Vol. 45, Feb. 197, pp. 228-238.

H. Davies, "Reflection of Electromagnetic Waves From A Rough Surface" IEE Monograph # 90 (1954)

R. K. Moore, "Resolution of Vertical Incidence Return into Random and Specular Components" UNM Eng. Ex. Sta. Tech Report, EE-6 (July, 1957)

F. Janza and R. West, "Accurate Radar Attenuation Measurements Achieved by Inflight Calibration," IRE Tran. on Instrumentation, pp. 23-30 (Oct. 1955).

R. A. Hessemer, Jr., and C. S. Williams, Jr., "Determination of Radar Cross-Section For a Scattering Ground," Sandia Corp. Tech. Memo 206-54-54 (Sept. 1954).

J. M. Usry and R. B. Glascock, "Converting Measured Antenna Patterns to Sperical Coordinates," UNM Eng. Ex. Sta. Tech. Report EE-3 (March, 1957).

C. Beard, I. Katz, and L. Spetner, "Phenomenological Model of Microwave Reflection From the Sea" IRE Trans. on Ant. and Prop. Vol. AP-4, No. 2 p. 142 (1956).

A. R. Edison, "Reflection and Scattering Coefficients for Several Types of Targets", UNM Exp. Sta. Tech. Report EE-8 (Sept. 1957).

Reference Data for Radio Engineers 4th Ed. p. 698 and p. 700 Int. Tel. and Tel. Co. 67 Broad St. New York 4, N. Y. (1956).

S. O. Rice, "Mathematical Analysis of Random Noise" B.S.T.J. Vol. 24, pp. 125, 126 (1945).

S. O. Rice, "Mathematical Analysis of Random Noise" B.S.T.J. Vol. 23, p. 312 (1944).

Peter D. Welch, "Progress Report on Interpretation and Prediction of Radar Terrain Return Fading Spectra", Physical Science Laboratory, Report AER 14W, New Mexico A. & M. A. College Station, New Mexico.

Samuel Silver, Editor, Microwave Antenna Theory and Design, Radiation Laboratory Serives, Vol. 12, (McGraw-Hill (New York, 1949) pp. 359-360.

Stanford Goldman, Information Theory, Prentise-Hall, Inc. (New York, 1955) pp. 223-224.

Paul Drude, Theory of Optics Longman, Green & Co. (London, 1913) p. 164.

Janza, Hessemer, & Williams, "Pulse Response of Terrain Return Receivers," Sandia Corp. Tech. Memo. 208-54-54.